The Immitigable Nature of Assembly Bias: the Impact of Halo Definition on Environmental Effects

Antonio S. Villarreal,[1]* Andrew R. Zentner,[1]† Yao-Yuan Mao,[1]‡
Christopher W. Purcell,[2]§ Andrew P. Hearin,[3]¶ Frank C. van den Bosch,[3]‖
and Benedikt Diemer[4]**

[1] *Department of Physics and Astronomy & Pittsburgh Particle Physics,*
Astrophysics, and Cosmology Center (Pitt-PACC),
University of Pittsburgh, Pittsburgh, PA
[2] *Department of Physics and Astronomy,*
West Virginia University, Morgantown, WV
[3] *Department of Astronomy,*
Yale University, Hew Haven, CT
[4] *Center for Astrophysics,*
Harvard University, Cambridge, MA

16 March 2017

ABSTRACT
Recent work has shown the importance of environment to the properties of dark matter halos. This brings conflict to standard implementations of the halo model and excursion set theory which assume that the properties of a population within the halo is determined by the mass of the halo alone. We seek to find a definition of the size of a halo that allows us to minimize the impact of assembly bias on halo model calculations. We analyze the dependence on environment of our properties using the method of marked correlation functions for several different halo definitions, utilizing the Diemer & Kravtsov (2015) simulations. We find that the strength of assembly bias has a strong dependence on the measured halo mass, even when using marks normalized around fixed mass. We note that differences in halo definition, sample selection, and properties of interest can greatly impact the measurement of assembly bias, potentially explaining conflicting results in the literature. These results suggest that halo assembly bias appears increasingly difficult to resolve using the definitions common in current halo finder techniques, possibly pointing toward the necessity of methods such as utilizing the halo splashback radius.

Key words: cosmology: dark matter – cosmology: large-scale structure of Universe – galaxies: formation –galaxies: halos – methods: numerical

[ARZ: We should add Andrew Hearin and Frank van den Bosch. Look into formatting the title correctly. Once I'm happy with the quality of the writing, we'll also need to send this to Benedikt Diemer and Andrey Kravtsov and offer them authorship.]

* E-mail: asv13@pitt.edu
† E-mail: zentner@pitt.edu
‡ E-mail: yymao@pitt.edu
§ E-mail: cwpurcell@mail.wvu.edu
¶ E-mail: andrew.hearin@yale.edu
‖ E-mail: frank.vandenbosch@yale.edu
** E-mail: benedikt.diemer@cfa.harvard.edu

1 INTRODUCTION

[ARZ: There is still a notation problem. In some parts of the text you use "L0125" etc. while in some parts, like Table 1, you use "low-mass", "mid-mass", etc. You have to choose one and go with it. If you like, you can say that the halo samples that you extract from the L0125 simulation will be referred to as "low-mass" and so on. That would be fine. However, you have to explicitly say that when you discuss your sample selections."] [ASV: My intent is to use "L0125" and the like to refer to the N-Body simulation and "low-mass" to refer to the mass cuts, though I understand the confusion. I made a pass to attempt to be more consistent with this.]

In the concordance cosmology, galaxies and clusters form within merging dark matter halos (White & Rees 1978; Blumenthal et al. 1984; Mo et al. 2010). Numerical simulations have provided a solid understanding of the abundances, properties, and clustering of dark matter halos in the standard cosmological model. Accordingly, it is possible to compute the clustering statistics of galaxies given a model for the (probabilistic) relationship between galaxies and dark matter halos. Such halo occupation models have been used to interpret large-scale structure measurements and constrain models of galaxy evolution (Yang et al. 2003; Tinker et al. 2005; Zehavi et al. 2005; Porciani & Norberg 2006; van den Bosch et al. 2007; Zheng et al. 2007; Conroy & Wechsler 2009; Yang et al. 2009; Zehavi et al. 2011; Guo et al. 2011; Wake et al. 2011; Yang et al. 2011, 2012; Leauthaud et al. 2012; Rodríguez-Puebla et al. 2012; Behroozi et al. 2013b; Moster et al. 2013; Tinker et al. 2013; Cacciato et al. 2013; More et al. 2013; Guo et al. 2014; Zu & Mandelbaum 2015). To date, the vast majority of halo occupation models rely on a key assumption, namely that the probability of a halo to host a number of galaxies of a particular type depends only upon halo mass. It is now well known that the clustering strength of halos depends upon properties such as halo formation time (Gao et al. 2005; Harker et al. 2006; Wechsler et al. 2006; Gao & White 2007; Croton et al. 2007; Zentner 2007; Dalal et al. 2008; Li et al. 2008; Lacerna & Padilla 2011), concentration (Wechsler et al. 2006; Faltenbacher & White 2010; Mao et al. 2015), and other halo properties (Bett et al. 2007; Hahn et al. 2007a,b; Faltenbacher & White 2010; van Daalen et al. 2012; Fisher & Faltenbacher 2016; Sunayama et al. 2016; Chaves-Montero et al. 2016). If galaxy properties depend upon these halo properties, a phenomenon known as galaxy *assembly bias*, then standard halo occupation modeling will fail (Zentner et al. 2014) and more complex models (Gil-Marín et al. 2011; Hearin et al. 2016b) are necessary.

In this work, we explore the possibility of simplifying halo occupation modeling, at least for some applications, by altering the definition of a halo. Traditional definitions of halo boundaries are not particularly well motivated, so it seems natural to explore alternative definitions of halo size. Halo definitions have become a matter of convention that vary considerably in the literature. Many authors define halos using a friends-of-friend (FoF) algorithm applied to the particle distribution that designates halo boundaries as regions of roughly constant density. More often, authors define halos by spherical overdensity (SO) regions within which the mean density exceeds a particular threshold. The threshold used varies significantly. With respect to the mean density of the universe, commonly used thresholds are 178, 180, 200, and ∼340 times the mean background density, the last of these being the "virial" overdensity in a concordance ΛCDM universe. Significantly higher values of the overdensity parameter are often used in studies of X-ray emission from cluster-sized halos.

Our work is an attempt to use halo definition to work for the convenience of the practitioner. We study the strength of various halo assembly bias signals as a function of halo definition. This is motivated, in large part, by recent literature that suggests that a large portion of the assembly bias signals are driven by halos in the relatively dense environments surrounding larger halos (Wang et al. 2007; War-

nick et al. 2008; More et al. 2015; Sunayama et al. 2016). Moreover, the environmental impacts of halos on one another has been shown to extend beyond well beyond traditional virial radii. (Adhikari et al. 2014; Diemer & Kravtsov 2014; Wetzel et al. 2014; More et al. 2015; Wetzel & Nagai 2015) **[ARZ: Need citations here to work by Wang (2007), the recent work on splashback (backsplash) and flyby halos, and the recent work on the splashback radius.][ASV: Should be fairly complete here, but I'll do another round of looking over the literature to see if I have missed anything recent.]** Halos in dense environments (e.g., near other large halos) exhibit anomalous properties (e.g., formation times, concentrations, etc.) compared to field halos in part because of their interactions with their larger, neighbor halos. It seems interesting to ask whether or not defining halos to contain many of these anomalous neighbor halos, thus using the halo concept to draw a more meaningful boundary around regions within which highly nonlinear effects are important, can mitigate halo assembly bias. Assessing this strategy is the aim of our paper.

We restrict ourselves to halos that are defined by spherical regions and we study the strength of halo assembly bias as a function of the density threshold used to demarcate these halos. We find that for halo properties that measure the degree of central mass concentration, there exist halo definitions in which assembly bias may be greatly mitigated. However, the definitions which mitigate concentration-based assembly bias are mass dependent; high-mass, cluster-sized halos appear to have little assembly bias for a traditional overdensity definition of $\Delta \approx 200$, while low-mass halos ($\sim 10^{11} \, h^{-1} \mathrm{M}_\odot$) require $\Delta \approx 20$. Any mitigation strategy must be complex and mass dependent, as might be expected given the mass dependence of the assembly bias effect Wechsler et al. (2006). We find that we cannot mitigate the assembly bias of halos selected by properties other than concentration, such as halo spin, halo shape, and number of satellite halos. These results suggest that any mitigation schemes will likely be quite complex if it all practical. **[ARZ: I plan to add something here after I complete my run through the paper.]**

[ARZ: This paragraph makes no sense. I suspect there is some sort of editor problem. Please fix this.][ASV: Attempted a pass at fixing this up, not sure I am entirely happy with it as of yet.] In § 2 of this paper, we discuss the cosmological simulations and halo finders utilized in the analysis. In § 3, we discuss and define the halo properties used as our tracers of assembly bias. In § 4, we discuss the statistics that we use to measure environmental effects after halo redefinition. We also discuss our method of removing known mass scaling from halo properties. In § 5, we present our findings and consider how the change of halo definition impacts measures of assembly bias. In § 7, we discuss the significance of our results in the context of halo modelling. We also consider the nature of assembly bias as a function of halo definition.

2 SIMULATIONS AND HALO IDENTIFICATION

In order to study the effects of halo redefinition, we use three cosmological N-body simulations of structure formation. The Diemer & Kravtsov (2015) simulations each utilize a Planck best-fit cosmology with $\Omega_\mathrm{M} = 0.32$, $\Omega_\Lambda = 0.68$, and $h_0 = 0.67$. We use three simulation boxes with comoving sizes of 125, 250, and 500 $h^{-1}\mathrm{Mpc}$ respectively. The particle masses are 1.6×10^8, 1.3×10^9, and 1.0×10^{10} $h^{-1}\mathrm{M}_\odot$ respectively, implying a total of 1024^3 particles in each simulation. The three simulations have force softening scales of 2.4, 5.8, and 14 $h^{-1}\mathrm{kpc}$. We refer to each simulation as L0125, L0250, or L0500 for the remainder of the paper. This set of simulations allows us to probe the resolution effects inherent in halo finding (due to the varying resolutions of the simulations) and to probe the mass dependence of halo clustering over a wider range of halo masses than would be possible with only one simulation from the set. For example, L0125, with its higher resolution, contains the least massive resolved halos, while L0500 has the most robust statistics for the most massive halos as a result of the larger simulation volume.

To identify halos, we use the ROCKSTAR halo finder, which works on the phase space algorithm described in Behroozi, Wechsler & Wu (2013a). In short, ROCKSTAR determines initial groupings of particles using a Friends-of-Friends algorithm in phase space before applying the spherical overdensity halo definition in order to determine halo properties of interest. Unbound particles are removed prior to the calculation of halo mass and other halo properties. Our method of halo redefinition is to change how halo size is calculated as part of the ROCKSTAR pipeline. A halo is given a radius, r_Δ, determined by

$$\bar{\rho}(r_\Delta) = \Delta\rho_\mathrm{m}, \qquad (1)$$

where the mean density within a spherical volume of radius r is $\bar{\rho}(r)$, Δ is the overdensity parameter, and ρ_m is the mean background mass density of the simulation. The resulting halo size calculation can have a large variation depending on the choice of Δ. The number chosen for Δ varies throughout the literature from $\Delta \approx 178$ to $\Delta \approx 340$ or higher for X-ray studies of clusters. We choose to vary the size of a halo by treating the overdensity parameter as tunable, expanding the range from $\Delta = 340$ to $\Delta = 20$. While this range is greater than the differences between most the common overdensity choices, this broad range enables a fairly extensive exploration of environmental effects on halo properties as a function of halo definition[1].

An additional benefit of the ROCKSTAR software is the ability to identify substructure, commonly referred to in the literature as subhalos. Effectively, all density peaks are identified within the simulation and if a halo exists within the phase space of another halo, the less massive of the two is defined to be a subhalo of the more massive companion. This process continues until all halos have been assigned. For purposes of our calculations, we only use the immediate

subhalos of the host, as these are most likely to be associated with satellite galaxies and have the best connection to concrete observables. [ASV: Felt it was best to put in a small section describing how ROCKSTAR identifies subhalos in order to set up the discussion further.]

3 HALO PROPERTIES

As has long been well known, halo mass is the property that most strongly affects halo clustering. In this paper, we aim to study the strength of halo clustering as a function of halo properties other than mass. We will refer to these properties as "auxiliary" halo properties in this paper. The properties we study are described in this section.

3.1 Measures of Halo Concentration

We investigate the clustering of halos as a function of a number of halo properties that have been shown to influence halo clustering at fixed halo mass. We explore two definitions of halo concentration. The first stems from a fit of the spherically-averaged halo density profile, $\rho(r)$, to a Navarro et al. (1997); hereafter, NFW density profile,

$$\rho(r) = \frac{\rho_0}{\frac{r}{r_\mathrm{s}}(1 + \frac{r}{r_\mathrm{s}})^2}, \qquad (2)$$

where the density scale, ρ_0, and the scale radius, r_s, are parameters that are fit to the density profile of each halo. The standard definition of halo concentration is then

$$c_\mathrm{NFW} = \frac{r_\Delta}{r_\mathrm{s}}, \qquad (3)$$

where r_Δ is the radius of the halo given an overdensity parameter, Δ, defining the halo and r_s is the inferred halo scale radius. We use the NFW concentrations computed by the ROCKSTAR halo finder, which are derived from a fit to the halo density profile.

The NFW concentration defined in the previous paragraph has the shortcoming that it depends upon a parametric description of dark matter halos, so we study the clustering dependence of halos as a function of a non-parametric description of halo concentration as well. In particular, we use the "velocity-ratio" concentration,

$$c_\mathrm{V} = \frac{V_\mathrm{max}}{V_\Delta}, \qquad (4)$$

where V_max is the maximum circular velocity achieved within the halo and V_Δ is the circular velocity at the halo radius, r_Δ. All halos of the same mass have the same value of V_Δ; however, they exhibit a variety of V_max values depending upon the degree to which their masses are concentrated toward the halo center. The quantity c_V is a non-parametric measure of halo concentration and can be measured from simulation snapshots without fitting halo density profiles. Consequently, c_V is robust to halo density profile parameterizations and halo profile fitting procedures.

Halo concentrations are interesting to investigate for these purposes for a number of reasons. First of all, the environment dependence of halo concentrations is known to be strong for standard halo definitions. Second, halo concentrations are of interest in the modeling of galaxy clustering and gravitational lensing statistics (and their cross correlations).

---

[1] It is worth noting that the ROCKSTAR linking length parameter must be adjusted as Δ varies in order to ensure that SO halos contain all relevant particles.

In the case of galaxy clustering, the relevance is indirect, because galaxies may not trace the mass densities of their host halos. In the case of gravitational lensing, the mass distribution is the primary quantity of interest and halo concentrations are directly related to predictions for lensing statistics. Third, concentrations can be measured from individual simulation snapshots easily and halo concentrations are known to be strongly correlated with the formation histories of dark matter halos with earlier forming halos having higher concentrations at fixed halo mass (Wechsler et al. 2002; Zhao et al. 2003; Wechsler et al. 2006; Zhao et al. 2009). As such, exploring the concentration dependence of halo clustering may yield insight into the age dependence of halo clustering without the need for constructing merger trees. This is particularly important in the present study in which the halo finding is performed repeatedly for many different values of Δ. Constructing a self-consistent merger tree from which halo formation history can be studied requires halo finding at all simulation snapshots for each new value of Δ, which is a computationally prohibitive task.

In the present paper, we limit our study to halo properties that can be measured from a single simulation snapshot. However, halo formation histories correlate with halo concentrations with significant scatter and this correlation may depend upon environment, so the reader should be wary of drawing conclusions about the environmental dependence of halo formation by extrapolating our results on halo concentration. We will explore measures of halo age directly in a forthcoming follow-up study dedicated to halo formation histories.

[ARZ: There should be uniformity in your presentation in Figures 1 and 2. Right now, they present nearly identical information in different ways. I personally find Fig. 2 easier to read, so I would make the other figures follow that model. The only thing I would add is to color code the arrows as well. Then adjust the text accordingly.] Figure 1 shows the mean c_{NFW}-M_Δ relation for halos defined with $\Delta = 200$ in L0125, L0250, and L0500. For each simulation, we consider halos only above a minimum mass threshold to ensure that property measurements are not compromised by resolution effects. The minimum mass thresholds are shown as the vertical lines in Fig. 1 and listed in Table 1. Similar to Fig. 1, Figure 2 shows the relation between the velocity-ratio concentration, c_{V}, and halo mass. In the interest of completeness, Figure 3 shows the relationship between c_{NFW} and c_{V} on a halo-by-halo basis. As is evident, the two concentration proxies are strongly correlated and exhibit a $\sim 6\%$ scatter indicating that c_{NFW} and c_{V} indeed encode similar information about each halo.

3.2 Halo Shape

In addition to halo concentrations, we examine halo clustering as a function of a variety of other halo properties. We study halo clustering as a function of halo shape, s, quantified by the ratio of the halo minor, c and major axis, a, lengths,
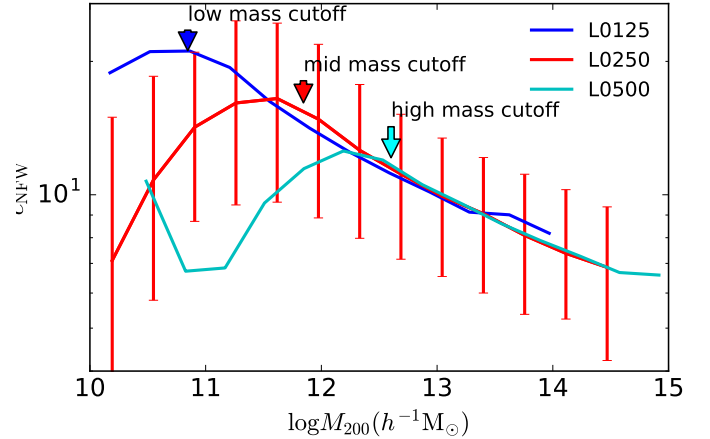
$$s = \frac{c}{a}. \tag{5}$$

Figure 1. [ARZ: Can you try making this a log-log plot? Does it look better or worse?] The relationship between the NFW concentration and halo mass for each of our simulations with $\Delta = 200$. In order of increasing simulation volume, the blue line corresponds to the concentration-mass relation from simulation L0125, the red line corresponds to L0250, and the cyan line corresponds to L0500. The red error bars show the 68% spread in parameter values within that mass bin for L0250. These errors are comparable to those of the other simulations within the region of interest. Each simulation is subject to resolution limitations at different halo masses. We show with arrows the minimum M_{200} mass thresholds that we adopt in our analyses using the same color code as the concentration-mass relations, going from L0125 to L0500 from left to right. Note the deviation from a monotonic trend as a result of resolution effects.

The halo shapes we used were measured with ROCKSTAR by calculating the mass distribution tensor for all particles within the halo radius, excluding identified substructure. The sorted eigenvalues of the matrix represent the squares of the principal ellipsoid axes, where a >b >c. [ARZ: Now you need to put a sentence or two in here about how shapes were measured. If you refer to Rockstar that is fine. But in that case put at least one or two sentences describing what Rockstar does to measure halo shapes.][ASV: Not sure if I should include the equation for the mass distribution tensor.] The mean relations for halo shapes as a function of halo mass for $\Delta = 200$ are shown in Figure 4 along with the mass thresholds used to ensure that our results are not compromised by resolution.

3.3 Halo Spin

We study halo clustering as a function of halo angular momentum quantified by the spin parameter, λ, as introduced by (Peebles 1969),

$$\lambda = \frac{J\sqrt{|E|}}{GM_\Delta^{2.5}} \tag{6}$$

where J is the halo angular momentum, E is the total energy of the halo, and M_Δ is the mass at the halo radius, r_Δ. We measure this quantity using ROCKSTAR which calculates the angular momentum, total energy, and total mass within Δ using bound particles out to the corresponding
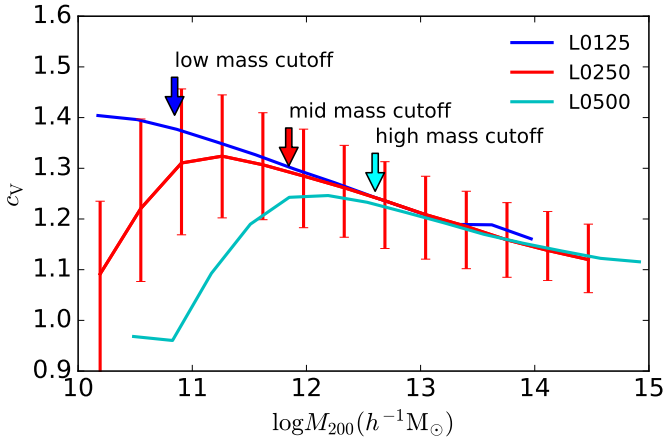
Figure 2. The relationship between the velocity ratio concentration and halo mass for each of our simulations with $\Delta = 200$. In order of increasing simulation volume, the blue line corresponds to the concentration-mass relation from simulation L0125, the red line corresponds to L0250, and the cyan line corresponds to L0500. The red error bars show the 68% spread in parameter values within that mass bin for L0250. These errors are comparable to those of the other simulations within the region of interest. Each simulation is subject to resolution limitations at different halo masses. We show with arrows the minimum M_{200} mass thresholds that we adopt in our analyses using the same color code as the concentration-mass relations, going from L0125 to L0500 from left to right. Note the deviation from a monotonic trend as a result of resolution effects.
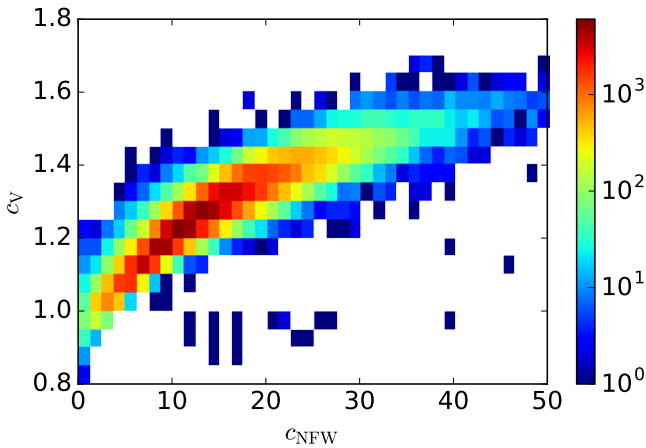

Figure 3. The relationship between the two different measures of concentration, using halos in L0250. The color scale, shown at the right, encodes the number of halos within a single two-dimensional bin in the c_{NFW}-c_{V} space. The red (blue) regions on the plot show where the most (fewest) halos exist with those values of the two concentration parameters. The white regions indicate where no halos hold these values. The scatter on this relationship ranges from 5% for intermediate concentration values, to a high of 13% at high masses.
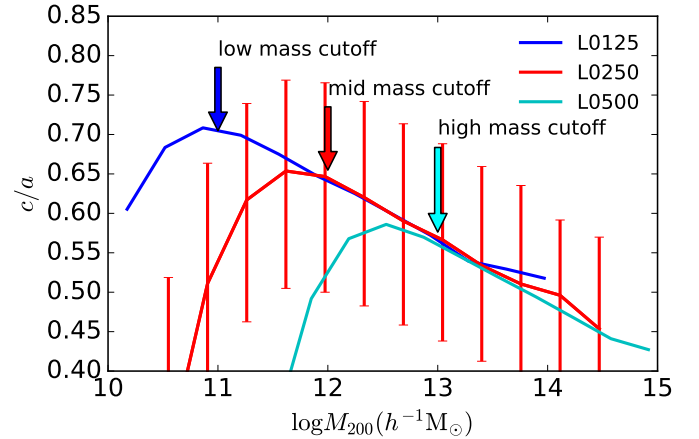

Figure 4. The relationship between the halo shape and halo mass for each of our simulations with $\Delta = 200$. In order of increasing simulation volume, the blue line corresponds to the shape-mass relation from simulation L0125, the red line corresponds to L0250, and the cyan line corresponds to L0500. The red error bars show the 68% spread in parameter values within that mass bin for L0250. These errors are comparable to those of the other simulations within the region of interest. Each simulation is subject to resolution limitations at different halo masses. We show with arrows the minimum M_{200} mass thresholds that we adopt in our analyses using the same color code as the shape-mass relations, going from L0125 to L0500 from left to right. The mass cutoffs chosen for this mark are at higher masses in order to account for the additional number of particles needed to properly measure the halo shape. Note the deviation from a monotonic trend as a result of resolution effects.

halo radius. **[ARZ: Brief note on how λ is measured. Again, this may refer to Rockstar, but put a sentence or two summarizing the Rockstar procedure.]** The mean relations for halo spin as a function of halo mass for $\Delta = 200$ are shown in Figure 5 along with the mass thresholds enforced to ensure that our results are not compromised by resolution. These thresholds are summarized in Table 1, where we also show the threshold masses at various values of the overdensity parameter, Δ.

3.4 Halo Samples

In practice, the mean relations between the various halo properties and the mass thresholds for our analyses must be determined separately for each combination of simulation, halo property (e.g., c_{NFW} or s), and halo definition (i.e., value of Δ in the case of the present study). For each analysis, we set mass thresholds in order to avoid the regime in which halo parameters are not well measured due to resolution limits of the simulations; we draw attention to the downturn in Figure 1 as an example of this, as the deviation from the underlying monotonic trend shifts with the change in simulation from lower to higher resolution, suggesting that this is the result of resolution alone.

For ease of comparison between halo definitions, we choose to use a single mass threshold for each simulation and value of Δ whenever possible, rather than on a parameter-by-parameter basis. The one exception to this method is the mass thresholds chosen for the halo shape parameter.
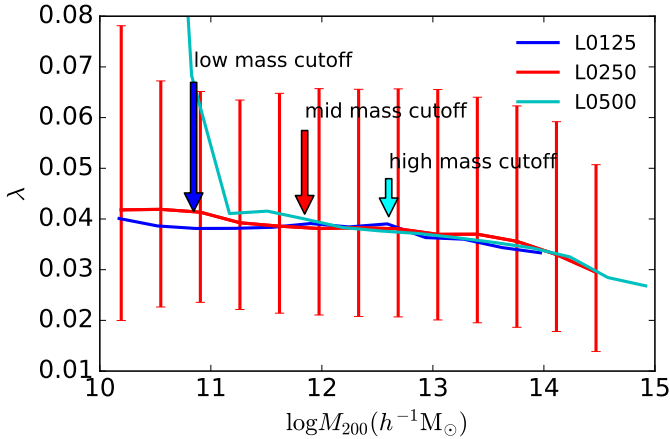
Figure 5. [ARZ: All of the same comments as for Fig. 1. Also, there is no reason here that the y-axis has to have such a large range. This crams all of the data into a small portion of the plot and makes most of the plot useless, wasted, white space. A more appropriate y-axis range looks to be from -0.1 to about 0.25 or so.] The relationship between the halo spin and halo mass for each of our simulations with $\Delta = 200$. In order of increasing simulation volume, the blue line corresponds to the spin-mass relation from simulation L0125, the red line corresponds to L0250, and the cyan line corresponds to L0500. The red error bars show the 68% spread in parameter values within that mass bin for L0250. These errors are comparable to those of the other simulations within the region of interest. Each simulation is subject to resolution limitations at different halo masses. We show with arrows the minimum M_{200} mass thresholds that we adopt in our analyses using the same color code as the spin-mass relations, going from L0125 to L0500 from left to right. Note the deviations from the near linear trend at low mass due to resolution effects.

This parameter requires a larger number of particles to be well measured; we direct attention to the downturn in Figure 4, which occurs at a significantly higher mass than demonstrated with other halo properties (see Figure 1 for comparison). [ARZ: than what? if you're making a comparison, you have to say what you are comparing it to.][ASV: Order of magnitude comment is removed since more recent Rockstar version allowed us to push down to lower mass in shape.] We analyze the shape parameter with separate, larger minimum mass thresholds to account for the requirement for a larger number of particles. This allows us to have better signal-to-noise in the remaining parameters, while avoiding drawing potentially erroneous conclusions when analyzing the halo shape parameter. We summarize the mass thresholds we have used for a subset of Δ values in Table 1. At most values of Δ, the minimum mass thresholds are driven by the requirement that the halo properties do not suffer significantly from finite resolution effects. We alert the reader to the fact that the mass of an individual halo will vary as Δ varies. This effect can be seen in Figure 6, which demonstrates that while a decreased value of Δ leads to larger masses on average, there is a scatter due to changes in halo identification. Roughly speaking, the threshold masses in Table 1 vary in such a way that the same physical objects are selected at each halo definition.
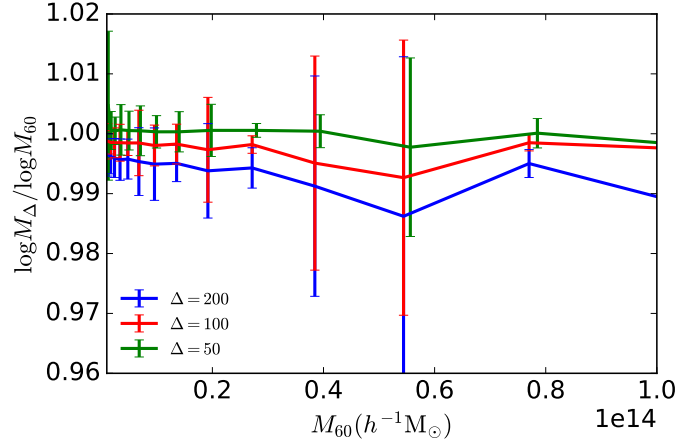
Figure 6. The ratio between host halo mass for a given definition of Δ and the equivalent halo for a definition of $\Delta = 60$ in logarithmic space. The blue (red, green) lines look at the ratio with respect to the values of $\Delta = 200 \, (100, 50)$. Note that while the expectation is that the halo mass will be larger for lower values of Δ, there are some differences due to differences in halo identification.

[ARZ: I though we discussed making a plot of M_Δ as a function of M_{200} for a few values of Δ and putting it in this section? I think that would be instructive for non-expert readers.] [ASV: Will do using the halo matched catalogs - in progress.] [ARZ: This still needs to be completed.][ASV: Added!]

4 HALO CLUSTERING AS A FUNCTION OF AUXILIARY HALO PROPERTIES

4.1 Auxiliary Halo Properties and Their Mass Dependence

We are interested in studying the clustering behavior of halos as a function of properties other than mass. As mass is the dominant halo property determining halo clustering strength and environment, we refer to the other properties that we study as "auxiliary halo properties" (those properties other than mass, such as concentration c_{NFW} or shape s). As has been demonstrated extensively in the literature, the auxiliary properties that we consider are themselves a function of mass (Bullock et al. 2002; Allgood et al. 2006; Duffy et al. 2008; Despali et al. 2016). This mass dependence, if not accounted for, induces auxiliary-property-dependent halo clustering. Most contemporary cosmological N-body simulations, and specifically the suite of simulations that we study in this work, do not have a sufficiently large number of halos to make isolating halos of fixed mass, and then further splitting these halos by an auxiliary property, a statistically powerful method with which to study the dependence of clustering on auxiliary properties. Therefore, it is necessary to remove and/or mitigate the mass dependence of the auxiliary properties that we study.

We mitigate the mass dependence of the auxiliary properties as follows. First, we take all host halos more massive than our minimum mass thresholds and sort them by their halo masses, M_Δ. We place these halos into twenty

Table 1. Minimum mass thresholds for each of our analyses. In the columns below each value of Δ, we show the minimum host halo masses considered in units of $h^{-1}M_\odot$. Those rows without a label of "-shape" refer to the mass cut chosen for all analyses other than halo shape. Those rows with a label of "-shape" refer to the mass cut chosen for the shape parameter analyses. The latter require higher mass thresholds.

Cutoff Name	$\Delta = 340$	$\Delta = 200$	$\Delta = 100$	$\Delta = 75$	$\Delta = 50$	$\Delta = 10$
low mass	6×10^{10}	7×10^{10}	8×10^{10}	9×10^{10}	1×10^{11}	2×10^{11}
low mass-shape	2×10^{11}	2×10^{11}	2×10^{11}	2×10^{11}	2×10^{11}	2×10^{11}
mid mass	6×10^{11}	7×10^{11}	8×10^{11}	9×10^{11}	2×10^{12}	N/A
mid mass-shape	2×10^{12}	2×10^{12}	2×10^{12}	2×10^{12}	2×10^{12}	N/A
high mass	3×10^{12}	4×10^{12}	5×10^{12}	6×10^{12}	7×10^{12}	N/A
high mass-shape	1×10^{13}	1×10^{13}	1×10^{13}	1×10^{13}	1×10^{13}	N/A

logarithmically-spaced bins of halo mass, ensuring that no bin has fewer than 10 halos, with the exception of the most massive bin. The objects in this final bin are rare and exceptional enough that they have little statistical value in the calculation process. [**ARZ: We need some number here or this needs to be rephrased.**][**ASV: So the last bin typically has a halo that is high enough mass that no reasonable binning structure will get that bin up to 10 halos with evenly spaced bins.**] We then calculate the rank of each mark within the bin of halo mass, from 1 to N, where N is the number of halos assigned to a given bin. If multiple halos share mark values (e.g. rank 2 and 3 have the same halo shape), then the average value is assigned as the mark (e.g. 2.5 to each). We normalize the marks between 0 and 1 by dividing out the number of halos in the bin, assuring that the distribution of marks within a bin fits a uniform distribution. This removes the strong mass trend in each of these properties. We use these new measures of halo auxiliary properties, those with the mean mass trend removed, to study halo clustering strength in the remainder of this work. We have experimented with different choices in property binning for defining the marks. We find that our qualitative results are not sensitive to the number of bins we use. Furthermore, the choice of equally populated bins versus evenly spaced bins makes no significant difference in the results. [**ARZ: You should make sure that your results do not change qualitatively under a few modifications. First, make sure that if you use finer binning that nothing qualitative changes (small quantitative changes can be acceptable). We have to be sure that our results are not sensitive to the number of bins that you choose here. Second, you should make sure that your results are not qualitatively different if you use medians rather than means. Third, I believe that you also explore removing the mass trend by removing a best fit power law $c(M)$ (or $s(M)$ or $\lambda(M)$ or whatever) relationship? If so, that is great. You should conclude this sentence with a statement along the lines of "We have experimented with a variety of methods to remove the gross mass dependence of these auxiliary properties and have verified that our qualitative results are not sensitive to the number of bins we use or the choice of median or mean property. Further, we have experimented with removing the gross mass dependence**

of auxiliary halo properties by subtracting away a best-fit power law relation for the property of interest and again, we find that our qualitative results are not altered using this method." We have to be able to give the reader some sort of confidence that our results are not driven by these seemingly arbitrary choices.] [**ASV: I'm not necessarily comfortable with the current ten bin situation and could conceivably switch back to equally populated bins, which allows for more total bins with halos to look at, but unevenly spaced in log mass.**] [**ARZ: This issue is important and unresolved. You must resolve it before we can move on. I don't understand why this important issue has been left unresolved during this last iteration of the draft?**] [**ASV: This was tested and I did not come back to changing my comment. We are still using equally populated mass bins, but it does not seem to qualitatively change our results. While I do not have one at the moment, making a comparison plot for two different bin sizes is pretty straightforward. Should I make a plot of that for the paper, or leave it for the referee process if needed? I also am not currently using the power law implementation, since I did not wish to worry about choice of interpolation method, but I certainly could whip that together pretty quickly, if still desired.**][**ASV: Changed to address our new method of using rank as our mark.**]

In addition to the properties of the host halos described in the previous section, we also study the strength of halo clustering as a function of subhalo number. Host halo size and the number of satellite halos (above some threshold in a proxy of satellite halo size) are also strongly correlated. Roughly speaking, the number of satellite halos above a fixed size threshold grows in approximate proportion to host halo mass (e.g., Zentner et al. 2005).

To account for the correlation between halo mass and abundance of subhalos, we follow the prescription of Wechsler et al. (2006). We first select all subhalos from the sample that meet the criteria that the ratio $V_{\max,\mathrm{sub}}/V_{\max,\mathrm{host}} \geq 0.3$, where $V_{\max,\mathrm{sub}}$ and $V_{mathrmmax,host}$ are the maximum circular velocities of the subhalos and host halos respectively. This choice of scaling exploits the fact that the subhalo velocity function is a very nearly self-similar function (Zentner et al. 2005) so that the scaling eliminates the gross

mass dependence of satellite number. [**ASV: need to add in additional citations here.**] In addition, this choice of threshold will mean that for subhalos above the resolution threshold of the simulation, there shall be of order one satellite halo per host on average. We then choose a cutoff in the max circular velocity such that all subhalos are well-resolved in the simulation volumes: $135, 235$, and $400 \mathrm{km \, s^{-1}}$ for L0125, L0250, and L0500 respectively. Subhalo maximum circular velocities were used as a proxy for subhalo size rather than subhalo masses because subhalo maximum circular velocities can be more robustly measured from simulation data, making comparison to other work easier. Once these cuts have been applied, we again divide the halos that meet these cutoffs into bins in logarithmic halo mass and follow the same procedure as with the other auxiliary halo properties. [**ARZ: I still don't understand this last choice in relation to the figures in the next section. For satellite number, you are selecting hosts above a Vmax threshold. I get that. But why is there a fixed Vmax threshold for each simulation? The L0500 simulation CERTAINLY CANNOT BE UN-AFFECTED BY RESOLUTION for satellites with $V_{\mathrm{max}} \sim 72 \, \mathrm{km/s}$, as your criteria require. So, either you are still doing something invalid here or I don't understand, which means the text needs to be modified.**] [**ASV: I agree with that and will give this a second lookover. I attempted to mimic the requirements of the Wechsler paper, but it does feel odd that there would be no resolution effects for the largest simulation. The only thing that might balance it out is the fact that it is still being hit by the first cut on host halos, but I do not think that should significantly increase the host halo circular velocities enough to counteract this effect.**] [**ASV: And comments addressed.**]

4.2   Clustering Statistics

We assess the influence of assembly bias specifically on two-point statistics of host halos. In order to do so, we study both the standard two-point correlation functions of halos selected by properties other than mass (e.g., the auxiliary properties concentration, shape, and spin) as well as halo mark correlation functions (MCFs). MCFs quantify the manner in which a halo property (the "mark") correlates among halo pairs as a function of the distance between the pairs. MCFs have the advantage that they effectively stack signal from all values of the halo auxiliary property, or mark, in contrast to selecting subsets of halos based on the auxiliary property. MCFs also stack signal from all environments and do not require any specific definition of halo environment in order to detect "environmental" trends that are usually referred to as assembly bias in the literature. Absent halo assembly bias, the halo marks are uncorrelated among pairs. MCFs have been used in many previous papers to quantify environmental dependence of halo properties other than mass (Sheth & Tormen 2004; Sheth 2005; Harker et al. 2006; Wechsler et al. 2006; Mao et al. 2015). Although it does not necessarily have to be the case, we find that using correlation functions of halo sub-samples and using MCFs lead to the same broad conclusions.

For a specific halo property, or mark m, we use the MCF

normalization of Wechsler et al. (2006), namely

$$\mathcal{M}_m(r) \equiv \frac{\langle m_1 m_2 \rangle_p(r) - \langle m \rangle^2}{\mathcal{V}(m)}, \qquad (7)$$

where m_i is the value of the mark for halo i, $\langle m \rangle$ is the mean of the mark, and $\mathcal{V}(m)$ the variance of the mark. The notation is intended to indicate that the average is taken over all pairs of halos separated by a distance r. In the absence of any correlation between a halo property among neighbors a separation r away, $\mathcal{M}_m(r) = 0$. Deviations of the MCF from zero indicate such correlations exist and the magnitude of $\mathcal{M}_m(r)$ gives the excess of the mark among pairs compared to the one-point mean of the mark $\langle m \rangle$ in units of the one-point variance. Given that our marks are distributed in a uniform distribution from 0 to 1, we anticipate that $\langle m \rangle^2 = 0.25$ and that $\mathcal{V}(m) = 1/12$.

The marks that we use throughout our calculations are the ranks of the halo NFW-defined concentration, halo velocity ratio, halo shape, halo spin, and halo satellite number; in each case this serves to correct the underlying mass trends in these parameters as detailed in Section 4.1.

In each case, it is necessary to assess statistical fluctuations in the statistics that we measure in these simulations in order to determine the significance of the signals. For two-point correlation functions, we determine the covariance of the measurement through jackknife resampling of the eight octants of the simulation cube. We assess the significance of the MCFs by taking advantage of the inherent uniform distribution. For each radial bin in the marked correlation function, we determine the number of pairs, n, and draw from a uniform distribution n times to calculate the value of the marked correlation function in each bin. We then determine the 2% and 98% of the resulting randomizations; if the actual MCF signal lies within these two values, it is suggestive of a nondetection of assembly bias. We note that since we investigate the product of two uniformly distributed variables, a negative value of the MCF has two different interpretations. One interpretation is that halos with high (low) values of the mark experience enhanced (diminished) clustering. The other possible interpretation is an enhanced clustering of high value marks with low value marks. While we cannot distinguish between these two possibilities, it does not impact our ability to make statements about a potential non-detection of assembly bias, as our randomization implicitly accounts for the impact of a uniform product distribution.

5   RESULTS

5.1   Correlation Functions

We begin by studying the correlation functions of halos in our mass threshold samples, sub-selected by auxiliary properties. Figure 7 exhibits the difference between the clustering strength of halos in the 20th percentile highest NFW concentrations and the halos with the halos that have the 20th percentile lowest NFW concentrations as a function of the overdensity parameter, Δ, used to define the halos. In order to make the differences more apparent, the two-point functions in Fig. 7 have been normalized by the clustering strength of the entire halo sample.

If the clustering strength of halos were independent of

halo concentration, we would expect the lines in Fig. 7 to cluster around zero (scattered about zero by finite sample size). The evident deviations demonstrate that halos of different NFW concentrations exhibit appreciably different clustering, a fact that is already well known and has been studied by a number of authors. Furthermore, it is clear that the strength and sign of assembly bias due to NFW concentration is strongly mass dependent for any fixed halo definition, a result that also agrees with the significant previous literature on halo assembly bias using conventional halo definitions (Wechsler et al. 2002; Gao et al. 2005; Zentner 2007; Wechsler et al. 2006; Harker et al. 2006; Croton et al. 2007; Dalal et al. 2008; Mao et al. 2015; Sunayama et al. 2016). At relatively low mass (the low-mass panel, $M_{200} > 7 \times 10^{10} \ h^{-1} M_\odot$), high-concentration halos are considerably more strongly clustered than low-concentration halos using the more conventional $\Delta = 200$ definition for halos. At somewhat higher halo masses (e.g., the mid-mass panel, $M_{200} > 7 \times 10^{11} \ h^{-1} M_\odot$), this difference is markedly reduced. Finally, for the highest-mass halos that we have the capability of studying (the high-mass panel, $M_{200} > 4 \times 10^{12} \ h^{-1} M_\odot$), the effect is weaker and also of opposite sign; low-concentration halos are more strongly clustered than high-concentration halos.

[ARZ: Did you ever run $\Delta = 70$ or $\Delta = 65$ like we discussed? If you make the plot color code based on the darkness of a single color, then I don't think we have to worry too much about making the plot look too busy.][ASV: It is run for $\Delta = 70$ and actually used for all our matching procedures with L0250. I can include that and see how we feel.] Focus, for example, on the middle panel of Fig. 7. In this panel, corresponding to the mid-mass threshold, the difference in large-scale clustering between high- and low-concentration halos is dramatically reduced for a halo definition with $\Delta \approx 60$ as compared to a more traditional halo definition, such as $\Delta = 200$. However, further decreasing Δ leads to concentration-dependent clustering of opposite sign. Both the strength and the sense of halo assembly bias depend upon halo definition! This is a point that may seem somewhat obvious in retrospect, but does not seem to be addressed explicitly anywhere in the literature despite its importance.

Comparing the differing clustering strengths across the three panels of Fig. 7, it is clear that any specific conclusions about concentration-dependent halo clustering vary with halo mass. For low-mass halos (the top panel), very low values of Δ (and correspondingly large definitions of halo radii, as R_Δ very roughly in proportion to $\Delta^{-1/3}$) are necessary in order to mitigate the concentration dependence of halo clustering. Conversely, for higher-mass halos (the bottom panel), conventional values of $\Delta \sim 200 - 340$ yield little concentration-dependent clustering. In this case, decreasing Δ (increasing R_Δ) results in significantly *increased* concentration dependent halo clustering. The reasons for these changes are of interest and we return to the interpretation of these results below.

Notice that in all panels of Fig. 7, the effect of concentration-dependent clustering is mildly scale-dependent. Moreover, this scale dependence is evident for all values of Δ. Simply defining halos with a different value of Δ does not suffice to eliminate concentration-dependent clustering on all scales. In this discussion and throughout,

we focus primarily on the large scale clustering, which we take to mean clustering on scales significantly larger than the radii, R_Δ of the halos in our samples.

It should be noted that this method is robust to the choice of samples. For instance, changing from examining the 20th percentile of concentrations to another value (e.g., 10th or 50th percentile) does not change the conclusions drawn from Fig. 7 significantly. In the case of halo concentration, adopting c_V rather than c_{NFW} also does not alter our conclusions. Therefore, we do not show these additional results in the interest of brevity.

Furthermore, we note that quite generally, for each of the halo properties we have studied, the conclusions drawn from examining correlation functions are the same as those drawn from studying MCFs. Consequently, we now move on to a more comprehensive discussion of the strength of auxiliary property-dependent halo clustering using MCFs.

5.2 Mark Correlation Functions

5.2.1 Halo Concentration

The NFW concentration, c_{NFW}, MCF is shown in Figure 8. The shaded bands in the figure delineate the statistical fluctuations in MCFs induced by finite sampling as discussed in Section 4.2. Qualitatively, Fig. 8 exhibits the same features that are evident in Fig. 7: more concentrated halos are significantly more clustered in the low-mass cut L0125 halo sample; concentration-dependent halo clustering weakens and reverses sense as halo mass increases (at fixed Δ), consistent with work on assembly bias (Wechsler et al. 2006; Sunayama et al. 2016); for the mid-mass cut L0250 sample with $\Delta = 60$, the large-scale concentration dependence of halo clustering has been reduced so as to be consistent with zero within the statistical limitations of the simulation. [ARZ: It seems like we need $\Delta \sim 65 - 70$ for L0250?][ASV: We have (or will have) the data from $\Delta = 70$, though it is not currently plotted due to cleanliness. I could always drop the $\Delta = 75$ in favor of it across the board.] [ARZ: I think if you make the color scheme change I'm asking for, cleanliness of the plot should not be a real issue.][ASV: Color change in!]

Figure 9 is a similar plot for the MCF of the velocity-ratio concentration, c_V. This figure exhibits qualitatively very similar features to Fig. 8, a fact that is not surprising given that we already know that c_{NFW} and c_V quantify largely redundant information about their halos. [ARZ: Any clue why the magnitude of the MCFs is much larger for c_V? I have one hypothesis that you should check. My hypothesis is that c_V is measured with less noise from the simulation data. You can check this in two ways. First, plot the one-point distribution (i.e., PDF) of the c_V mark and compare it to the one-point distribution of the c_{NFW} mark. If my hypothesis is correct, the PDF of c_V should be narrower and have few significant outliers. Second, show my the plot for the correlation functions (not MCFs) for a couple of percentiles of c_V. These should show an effect that is larger in magnitude. Show me both of these plots as soon as you can so I can write this interpretation here.]]asvThese plots will be hit in the next patch.
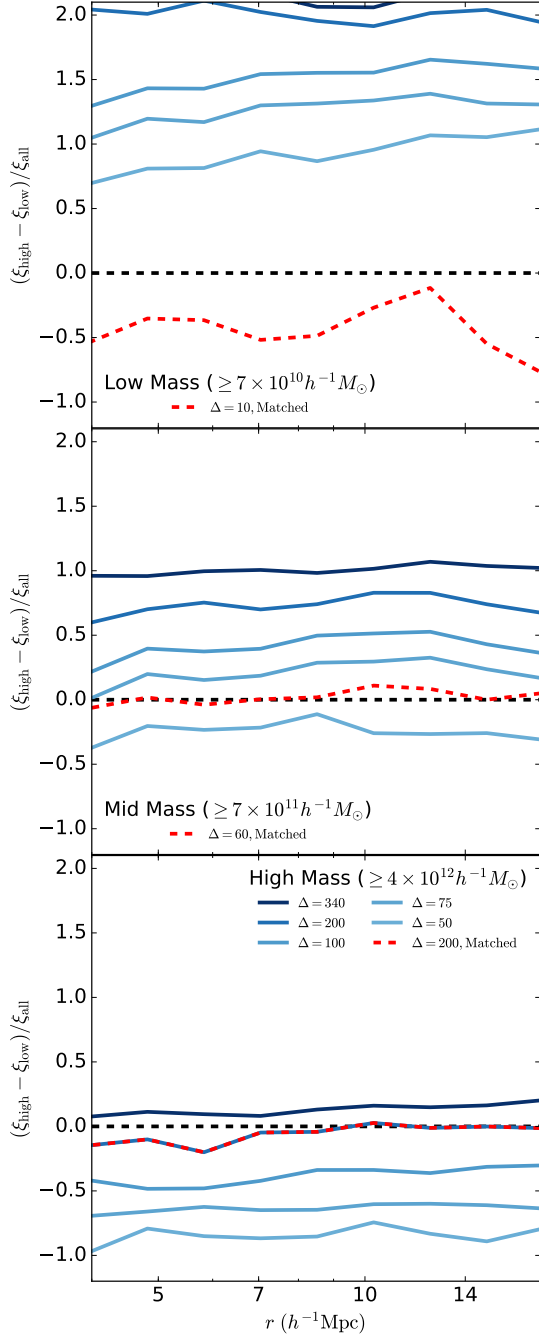
Figure 7. [ARZ: **The remaining problem with this plot is that each panel does not contain each line. This makes it very difficult to see which line corresponds to which value of Δ. Can you make sure that each value of Δ is represented on each panel? Otherwise labels for at least some of the values of the Δs will be needed. I have the same comment for each of the marked correlation function plots.**][ASV: **Fixed in most recent versions.**] In each panel, the solid lines plot the difference between the correlation function for the top 20% and the bottom 20% of halos by NFW concentration, normalized by the correlation function of the entire sample. In each plot the lines correspond to different values of Δ, with dark blue (light blue) corresponding to $\Delta = 340$ ($\Delta = 50$). The red dashed line corresponds to the overdensity chosen for matching as possibly removing assembly bias on most scales. The top (middle/bottom) panel shows the results for the L0125 (L0250/L0500) data set utilizing the low mass (mid mass/high mass) cutoffs

[ARZ: **Let's stick with these errors. They should be conservative.**]
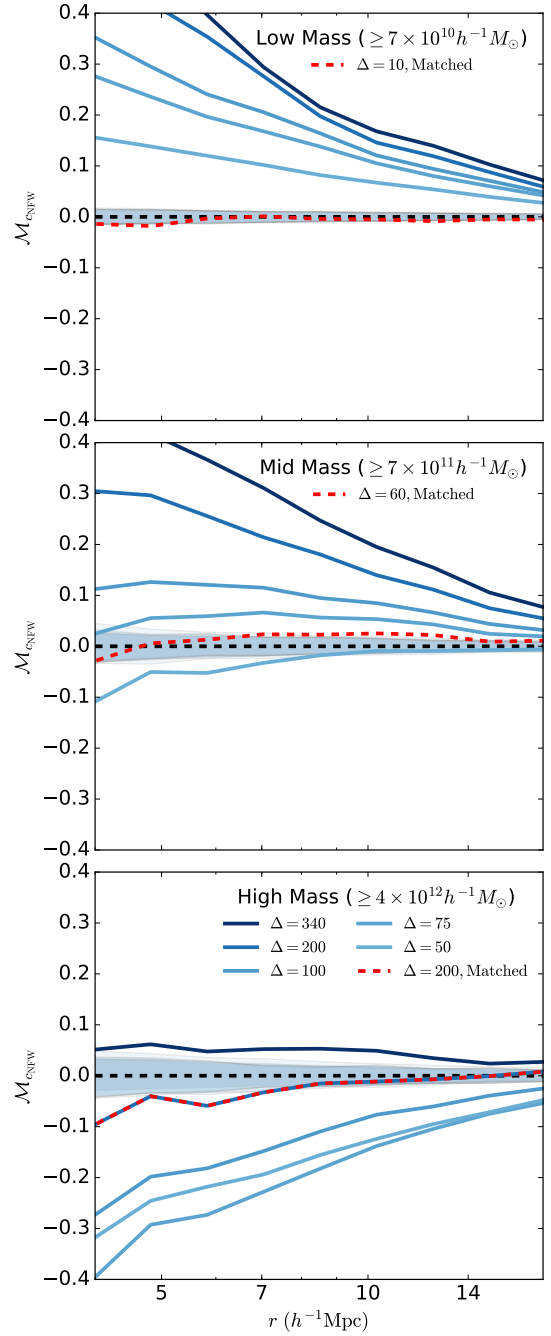
Figure 8. [ARZ: **Same comment as for Figure 6.**] The marked correlation function for the concentration defined according to the NFW profile. The solid lines plot the marked correlation function using NFW-defined concentration as the mark. In each plot the lines correspond to different values of Δ, with dark blue (light blue) corresponding to $\Delta = 340$ ($\Delta = 50$). The red dashed line corresponds to the overdensity chosen for matching as possibly removing assembly bias on most scales. The top (middle/bottom) panel shows the results for the L0125 (L0250/L0500) data set utilizing the low mass (mid mass/high mass) cutoffs. The shaded bands represent 2-sigma confidence regions generated by randomization of the marks.

I believe your hypothesis is correct from previous runs, but I will doublecheck to confirm

5.2.2 Halo Shape

Moving on from concentrations, Figure 10 illustrates MCFs in which the mark is the shape parameter, s, of the halo. Similar trends as the previous cases repeat themselves in the case where shape is used at the trace mark. For the entire range of halo masses studied, the fiducial halo definition shows enhanced clustering for the most spherical halos (halos with larger s values). Furthermore, our change in halo definition shows that increasing the size of halos (and decreasing Δ) leads to a reduction in this enhanced clustering.

Where the environmental dependence associated with the shape parameter distinguishes itself is in the best fit value of Δ for removing the halo assembly bias. No reasonable value of Δ seems to be capable of removing the enhanced clustering at the scales that we study, though the impact is reduced. This reduction may be driven by the filamentary nature of large-scale structure; increasing the volume assigned to any individual halo may only end up adding more filamentary structure to the halo that is not identified as substructure. This may result in smaller shape values that have enhanced clustering, serving to counteract the initial enhanced clustering at large shape values. Testing of this hypothesis is beyond the scope of this paper, but may well be testable through association of halos with large-scale structure.

[**ARZ: I don't understand what this is about? I don't see any reversal in trend? Has something changed?**] [**ARZ: I don't understand what any of this is about? What trend do you see that seems odd that you are trying to explain?**] [**ASV: Older versions of Rockstar had an error in determining shape that was leading to strange behavior. This newer version does not seem to have this and matches up better with existing literature.**]

5.2.3 Halo Spin

The spin MCFs are shown in Figure 12. Qualitatively, spin-dependent halo clustering is quite similar to shape-dependent halo clustering. Halos of high-spin cluster more strongly than halos of low-spin. [**ARZ: Search the literature, particularly Brandon Allgood's papers and Andreas Faltenbacher whose names come to mind, for spin-dependent assembly bias. I'm trying to figure out if yours is the first paper to point this out.**][**ASV: Need to track down all the specific citations, but after changing our normalization method, it seems to match up better with existing texts.**] Likewise, increasing halo radii by decreasing Δ in halo definitions only drives spin-dependent halo clustering to be stronger.

5.2.4 Subhalo Abundance

The clustering of halos as a function of the number of satellite galaxies at fixed mass is of particular practical interest. Efforts to model survey data on the large-scale galaxy distribution, such as the halo occupation distribution (HOD) or
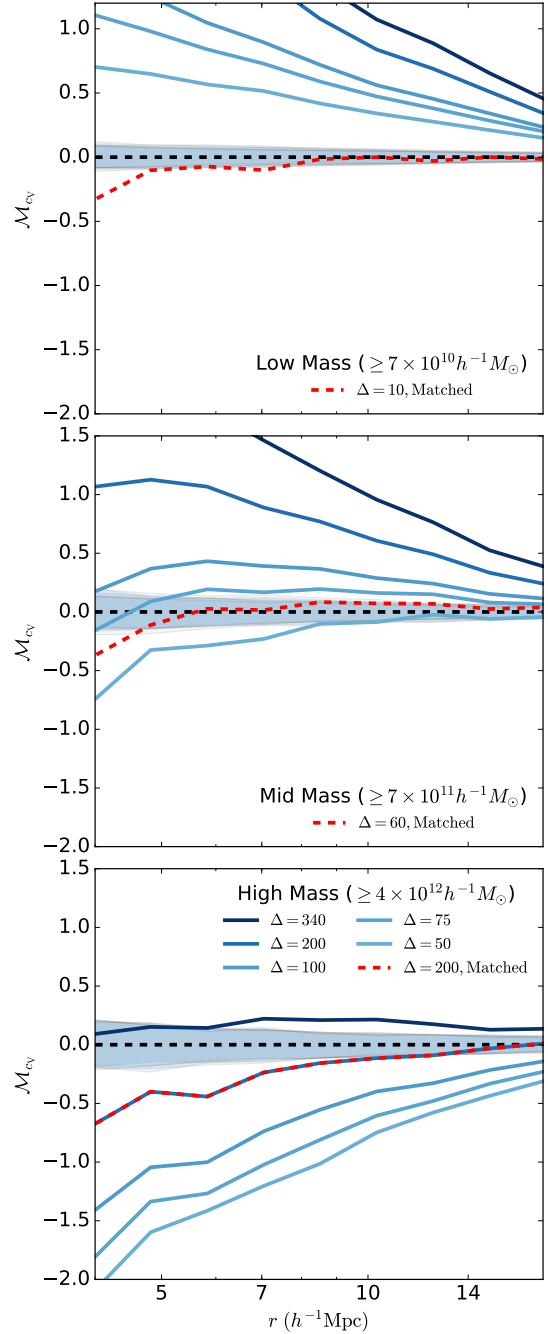

Figure 9. [**ARZ: Same comment as for Fig. 6.**] The marked correlation function for the concentration defined according to the ratio of max circular velocities. The solid lines plot the marked correlation function using velocity ratio concentration as the mark. In each plot the lines correspond to different values of Δ, with dark blue (light blue) corresponding to $\Delta = 340$ ($\Delta = 50$). The red dashed line corresponds to the overdensity chosen for matching as possibly removing assembly bias on most scales. The top (middle/bottom) panel shows the results for the L0125 (L0250/L0500) data set utilizing the low mass (mid mass/high mass) cutoffs. The shaded bands represent 2-sigma confidence regions generated by randomization of the marks.
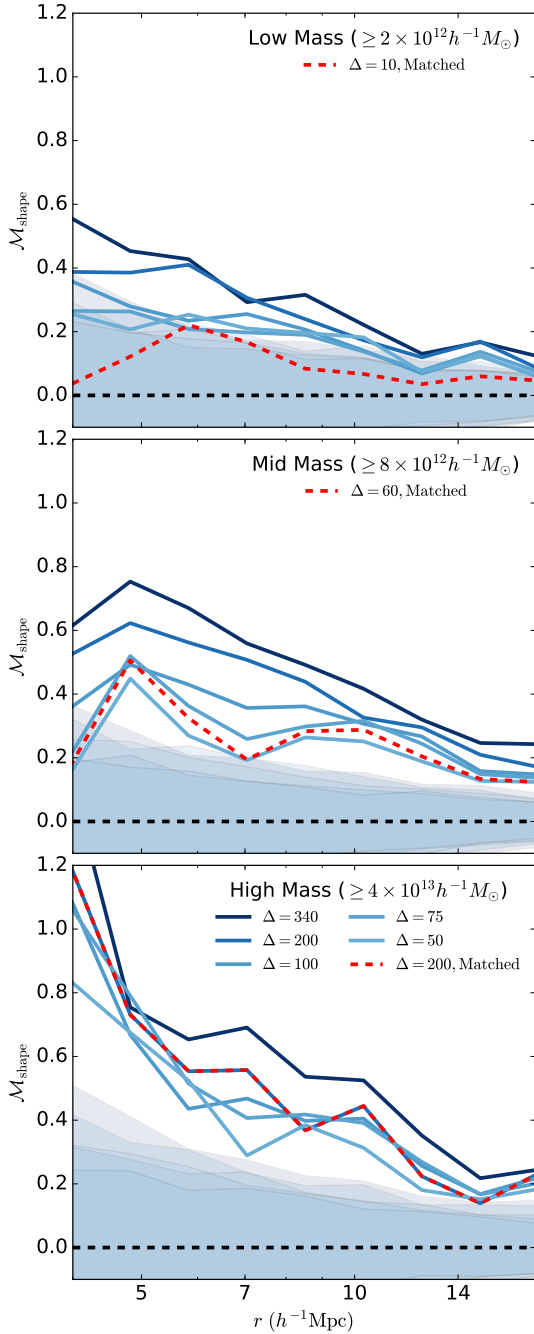
**Figure 10.** [ARZ: Same comment as for Fig. 6.] [ARZ: It looks like we still need $\Delta = 10$ line in the mid-mass and low-mass panels as well, just to be sure.] The marked correlation function for the halo shape parameter. In each plot the lines correspond to different values of Δ, with dark blue (light blue) corresponding to $\Delta = 340$ ($\Delta = 50$). The red dashed line corresponds to the overdensity chosen for matching as possibly removing assembly bias on most scales. The top (middle/bottom) panel shows the results for the L0125 (L0250/L0500) data set utilizing the low mass-shape (mid mass-shape/high mass-shape) cutoffs. The shaded bands represent 2-sigma confidence regions generated by randomization of the marks.
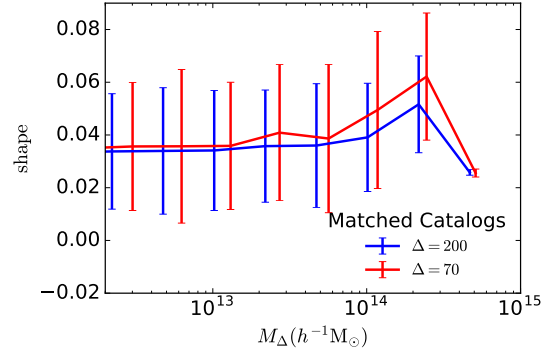
Figure 11. A comparison of the mean value of the halo shape for halos matched across both the $\Delta = 200$ and $\Delta = 70$ catalogs for L0250. The blue (red) line shows the mean value and scatter of the mean for the $\Delta = 200$ ($\Delta = 70$) catalog. Note that there is no significant increase in the scatter of the mean due to the change in halo definition.

conditional luminosity function (CLF) formalisms typically make the assumption that the multiplicity of satellite galaxies within a host dark matter halo depends solely upon halo mass. If this assumption is violated, then the phenomenological modeling of galaxy clustering can be more complicated than in these simplest scenarios.

Figure 13 shows clustering marked by satellite number as described in § 4. For all values of Δ, halo clustering is strongly dependent upon satellite occupation at all masses. Interestingly, altering halo definitions as we have makes little difference to this dependence. In fact, defining halos to have larger radii (smaller Δ) generally makes the environmental dependence of halo clustering more significant. Of course, our results pertain to satellite halos, or subhalos, rather than satellite galaxies, so the connection to observations and how one might model observed galaxy clustering is indirect, yet suggestive. We also note that the fact that the clustering appears reduced at lower masses is qualitatively in agreement with the predictions from Wechsler et al. (2006).

6   DISCUSSION

[ARZ: Repeating this comment here because of its importance. Look in the literature to see if spin-dependent halo clustering has been measured in the literature before. Look at http://arxiv.org/abs/1207.4476.]

We have confirmed that for conventional halo definitions halo clustering strength is a strong function of "auxiliary properties" halo concentration (either measured through a fit to the NFW profile or assigned non-parametrically as the ratio of the maximum circular velocity to the virial velocity), halo shape, halo spin, and number of subhalos for host halos over a wide range of masses. These findings are consistent with the now significant literature on the subject subject of halo assembly bias. (Peacock & Smith 2000; Wechsler et al. 2002; Sheth & Tormen 2004; Gao et al. 2005; Zentner et al. 2005; Allgood et al. 2006; Harker et al. 2006; Wechsler et al. 2006; Croton et al. 2007; Dalal et al. 2008; Mao et al. 2015; Sunayama et al. 2016) [ARZ: Reit-
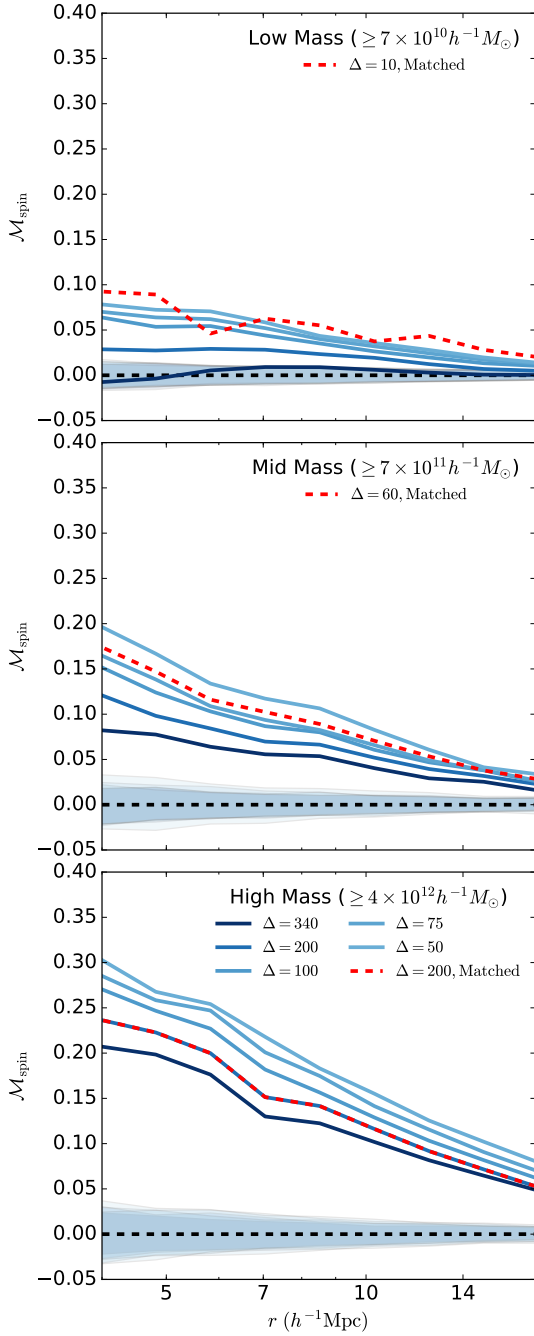
Figure 12. [ARZ: Same comment as for Fig. 6.] The marked correlation function for the halo spin parameter. The solid lines plot the marked correlation function using halo spin as the mark. In each plot the lines correspond to different values of Δ, with dark blue (light blue) corresponding to $\Delta = 340$ ($\Delta = 50$). The red dashed line corresponds to the overdensity chosen for matching as possibly removing assembly bias on most scales. The top (middle/bottom) panel shows the results for the L0125 (L0250/L0500) data set utilizing the low mass (mid mass/high mass) cutoffs. The shaded bands represent 2-sigma confidence regions generated by randomization of the marks.
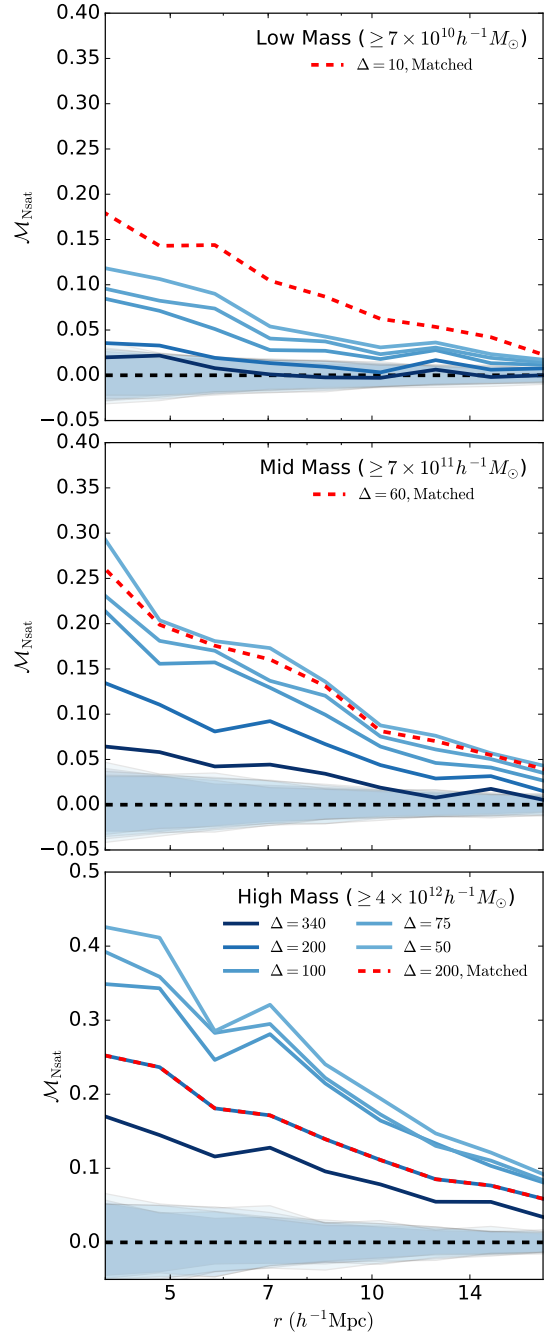
Figure 13. [ARZ: Same comment as for Fig. 6.] The marked correlation function for the satellite number parameter. The solid lines plot the marked correlation function using halo satellite number as the mark. In each plot the lines correspond to different values of Δ, with dark blue (light blue) corresponding to $\Delta = 340$ ($\Delta = 50$). The red dashed line corresponds to the overdensity chosen for matching as possibly removing assembly bias on most scales. The top (middle/bottom) panel shows the results for the L0125 (L0250/L0500) data set utilizing the low mass (mid mass/high mass) cutoffs. The shaded bands represent 2-sigma confidence regions generated by randomization of the marks.

erate citations here.][ASV: I THINK this covers our
bases, but my lit notes might be bad.]

We have explored the efficacy of alternative halo defini-
tions to mitigate the dependence of halo clustering on these
"auxiliary properties." Rather generally, we find that these
alternative definitions do *not* mitigate the effects of assem-
bly bias. In most cases, defining halos to have significantly
larger radii (lower Δ) than in conventional halo definitions
had only a modest influence on these assembly bias effects.
Moreover, to the degree that these modified halo definitions
had any effect at all, it was often of the sense of making the
assembly bias effect stronger, rather than weaker.

One exception to this general conclusion is the case of
halo concentration. Our results suggest that halo redefini-
tion may be able to mitigate concentration dependent halo
clustering. This is evident in Fig. 8 and Fig. 9. Halo con-
centration is strongly correlated with halo formation time,
so this suggests that such a redefinition may also aid in re-
ducing assembly bias associated with halo formation time;
however, this is a non-trivial extrapolation of our results and
a follow-up study to assess halo formation times in alterna-
tive halo definitions is both interesting and warranted.

Clearly, the halo definition that best mitigates
concentration-dependent assembly bias must be mass de-
pendent. Low values of Δ ($\Delta \sim 25$ with $R_{25} \sim 2R_{200}$) seem
appropriate near for our lowest mass-threshold sample (with
$M_{200} \geq 7 \times 10^{10}~h^{-1}M_\odot$) whereas $\Delta \sim 200$ or slightly
higher is adequate for our highest mass threshold sample
(with $M_{200} \geq 4 \times 10^{12}~h^{-1}M_\odot$). This result is reminis-
cent of much recent work on the so-called halo "splash-
back radius."(More et al. 2015) We note that while the splash-
back radius methodology does seem similar in concept to
our methodology, Fig. 14 demonstrates that a one-to-one
comparison between the two methods is difficult at best.
While both our method of halo redefinition and their de-
termination of splashback radius seem to show a monotonic
trend in mass, we note that our work with the lowest mass
halos requires a definition of halo radius that substantially
larger than the splashback radius method alone might sug-
gest. [ARZ: Here, compare our results to the splash-
back radius work.]

[ARZ: Here is where we could use ANOTHER
FIGURE! What I would like to see is a visual com-
parison of our "best" Δ as a function of halo mass
threshold compared to the equivalent for the splash-
back radius. To be clear, it is trivial to go back and
forth between Δ and radius (since radius $\propto \Delta^{-1/3}$)
so this can be represented with either Δ or radius. If
you choose to use radius, then it should probably be
normalized, such as R_Δ/R_{200} and $R_{\rm splashback}/R_{200}$ and
so on. This could be an important figure and point
to future work on this subject.] [ASV: Working on
creating this plot from the splashback radius paper.]
[ASV: New figure done and should be added in dur-
ing the next iteration with all new figures.][ASV:
And added.]

It is useful to investigate the reasons why halo redefini-
tions may be helpful in the case of concentrations. On the
positive side, it is possible that these redefinitions do define
halos an a more practically useful way, better isolating ob-
jects that have been strongly altered by nonlinear evolution
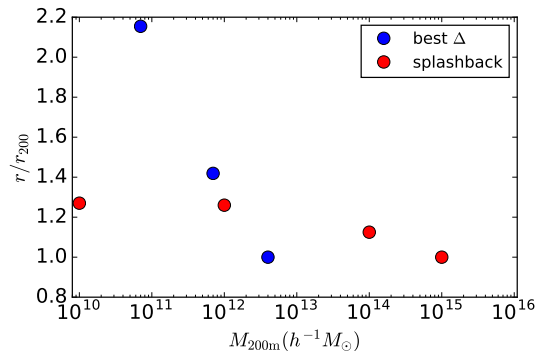from the larger-scale environment. In this case, halo redefi-

Figure 14. A comparison of the average ratio between r_{200} and
the splashback radius as determined by More et al. (2015) (red
circles) to the average ratio between r_{200} and the halo radius de-
termined as our best fit for removal of assembly bias as discussed
above (blue circles). Note that the halo mass chosen for the blue
points is determined by the mass cutoff in the simulation anal-
ysis, as the smallest (and most numerous) halos dominate the
calculation.

nition would be a step forward. However, it is also possible
that the details of measuring halo properties using these new
halo definitions introduce new sources of noise into the mea-
surements. If this is the case, then the reduction in environ-
mental effects stems from the fact that them measurement
of the halo property introduces noise and is *less* informa-
tive about the halo itself. For the case of halo concentra-
tion, which is the most interesting to follow up, introducing
noise can happen in numerous ways. For example, the NFW
concentration $c_{\rm NFW}$ is determined by a fit to the NFW pro-
file. Inferred values of $c_{\rm NFW}$ will depend upon the degree
to which the density profiles of the halos follow the NFW
functional form within some radius R_Δ that is different from
traditional halo radii, such as $\sim R_{200}$. At large halocentric
distances ($r \gtrsim R_{200}$) halo profiles are known to deviate from
the NFW form. It is worth noting that the velocity-defined
concentration c_V is a non-parametric measure of concentra-
tion and should be less subject to such effects.

[ARZ: New figure needed here. This should be,
for the L0250 simulation (my guess this one is most
instructive, but use your judgment here), a com-
parison of the concentration-mass relation for halos
defined with $\Delta = 200$ to the concentration-mass re-
lation for halos defined with $\Delta = 70$ (of whatever
you deem best). The figure must represent both the
mean (or median) relation AS WELL AS the disper-
sion in this relation at fixed mass. The plot should
exhibit this for both $c_{\rm NFW}$ and c_V. Two panels may
be necessary to make these points.] [ASV: contem-
plating how best to show this - currently making a
running median plot, as in the masscut plots above.]
[ASV: Figure is made and will be run on the new
dataset and included. It suggests that we are not sig-
nificantly changing the dispersion. Numbers added
below for now.]

As such, it is useful to examine the concentration-mass
relations for halos in the simulations for various halo def-
initions. This is shown in Fig. 15. Notice that the mean
dispersion of halo concentrations for a given mass bin are
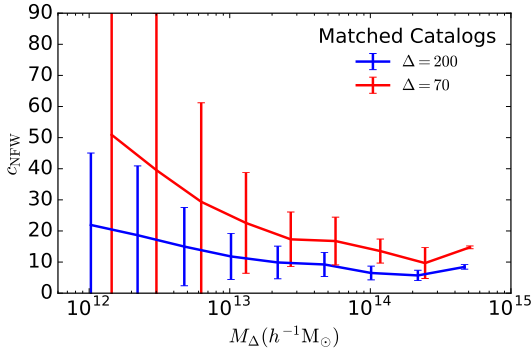not significantly changed as we move to our best fit value

Figure 15. A comparison of the mean value of the NFW-defined halo concentration for halos matched across both the $\Delta = 200$ and $\Delta = 70$ catalogs for L0250. The blue (red) line shows the mean value and scatter of the mean for the $\Delta = 200$ ($\Delta = 70$) catalog. Note that there is no significant increase in the scatter of the mean due to the change in halo definition.

of overdensity parameter, Δ. This is highly suggestive of the fact that the success of our method is not the result of larger measurement error, but is more fundamental to the nature of relating halo definition to our halo parameters of interest.[ARZ: Now you mention the interesting part about the new figure. This should be a discussion of how much larger/smaller the dispersion in concentrations gets for, say $\Delta = 70$ compared to $\Delta = 200$.] [ASV: The dispersion of halo concentrations is not significantly changed - while a little smaller, it is well within the scatter of the dispersion as well.]

We can explore in more detail the degree to which the mitigation of environmental effects by halo redefinition are due to introducing noise that is uncorrelated with environment into the measurement of halo properties when halos are defined in a manner distinct from the more traditional definitions. We proceed as follows. All host halos that are found in the halo catalogs constructed from lower values of Δ (for example, Δ 70 which is an interesting value for exploring concentration in the mid-mass cut of the L0250 simulation) are present as host halos in the halo catalogs constructed with higher values of threshold density (e.g., $\Delta = 200$). We match each halo in the lower threshold (lower Δ) simulation to its corresponding halo in the higher threshold catalog. We then consider the clustering of only those halos that we have matched across catalogs. We refer to these as the "matched" halo samples between two values of threshold overdensity Δ.

[ARZ: I removed the correlation function comparison here. It is too busy to read and not necessary. It also opens up the whole Pandora's box of "why choose 20%?" I'd rather avoid that in this discussion. Let's just jump straight to the MCF. This will reduce the proliferation of figures as well.][ASV: Seems entirely reasonable. I'm starting to see 5.1 as more of a proof of concept comparing to MCF results for those more comfortable working with 2pt functions.]

[ARZ: Please check to ensure that I know what you mean by your matched samples. Your language was not specific enough for me to be 100% sure. Modify as necessary.] [ASV: Looks absolutely correct to me.] Figure 16 shows the same statistic as Figure 8,
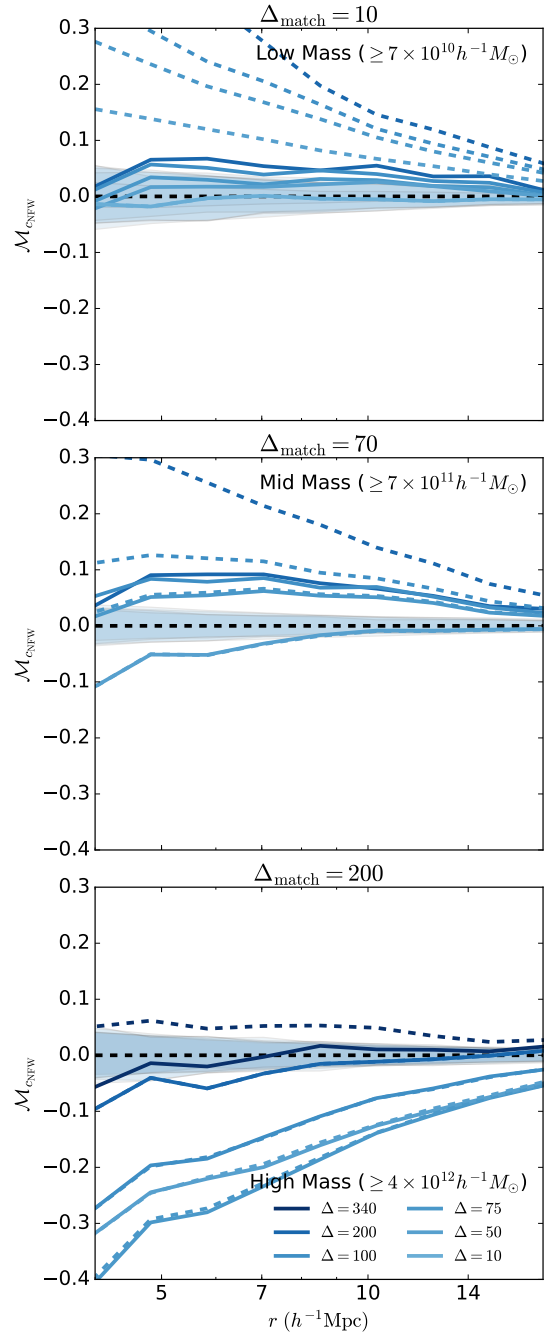

Figure 16. The marked correlation function for the NFW-defined halo concentration parameter. The solid lines plot the marked correlation function using NFW-defined halo concentration as the mark, for a catalog matched against the best fit Δ shown in red. The dashed lines plot the original marked correlation function results. In each plot the lines correspond to different values of Δ, with dark blue (light blue) corresponding to $\Delta = 340$ ($\Delta = 50$). The red dashed line corresponds to the overdensity chosen for matching as possibly removing assembly bias on most scales. The top (middle/bottom) panel shows the results for the L0125 (L0250/L0500) data set utilizing the low mass (mid mass/high mass) cutoffs. The shaded bands represent 2-sigma confidence regions generated by randomization of the marks. Only host halos consistent with the best-fit catalog from above are included in the analysis.

except for matched subsamples. The matched subsamples are matched to a catalog generated for the value of Δ most likely to remove assembly bias at large scales for the concentration marks; $\Delta = 10$ for the 'L0125-gen' cut, $\Delta = 70$ for the 'L0250-gen' cut, and $\Delta = 200$ for the 'L0500-gen' cut. These matched halo catalogs only differ from the standard halo samples in that they contain only those host halos common to both the catalog in question and the best fit Δ catalog. The most interesting matched sample to examine in this case is the $\Delta = 200$ sample. In this sample, all halos are defined as they would be defined in the $\Delta = 200$ catalog, including all inferred halo properties; however, the matched catalog contains only those host halos that also appear in the $\Delta = 70$ halo catalog. Therefore, many host halos have been removed from the sample because they have become subhalos in the $\Delta = 70$ catalogs.

From Fig. 16, it is apparent that some degree of assembly bias persists in the matched samples. Yet, what is interesting is that a very significant fraction of the assembly bias effect has been removed compared to the standard $\Delta = 200$ result. The halos in the matched catalogs have the same properties (including c_{NFW}) as those in the standard catalogs, so that removal of assembly bias is *not* due to introducing noise or other systematics into the measurement of concentration. That mitigation of assembly bias is due to the halo redefinition and, in particular, subsuming those halos most subject to assembly bias effects as subhalos of the $\Delta = 70$ halos. This is an interesting result suggesting that seeking optimal halo definitions may be one avenue to more completely separating the strongly nonlinear evolution occurring within halos from large-scale evolution and mitigating assembly bias.

[ARZ: Put a discussion of Fig. 17 here. It does not need to reiterate the discussion of Fig. 16. However, it should state that we reach the same broad conclusion and that this is good in part because c_V is a nonparametric measure of halo concentration.] Figure 17 follows the same exercise as above, with a comparison drawn to the Fig. 9. Notice that the same trends as Fig. 16 can be seen: a significant fraction of assembly bias is removed as compared to the unmatched catalog, though statistically significant assembly bias remains. Only in combination with halo redefinition do we remove assembly more completely on large scales. Note that the max circular velocity defined concentration is nonparametric by design; this helps to confirm that our result is not related to choice of halo density profile.

[ARZ: Would it be easy for you to plot the concentration-mass relation for only those host halos in the "matched" $\Delta = 200$ sample? If so, that would be potentially interesting for our interpretation.][ASV: In progress for above.]

[ARZ: This paragraph is good, but needs to be written a bit more professionally. Start with a sentence like, "It is interesting to explore the reasons that halo shape, spin, and satellite number are not amenable to having their assembly bias mitigated through simple halo redefinitions." Then move on to some specifics.] [ASV: attempted to rewrite more professionally!]

While halo shape, spin, and satellite number are not amenable to having their assembly bias mitigated through
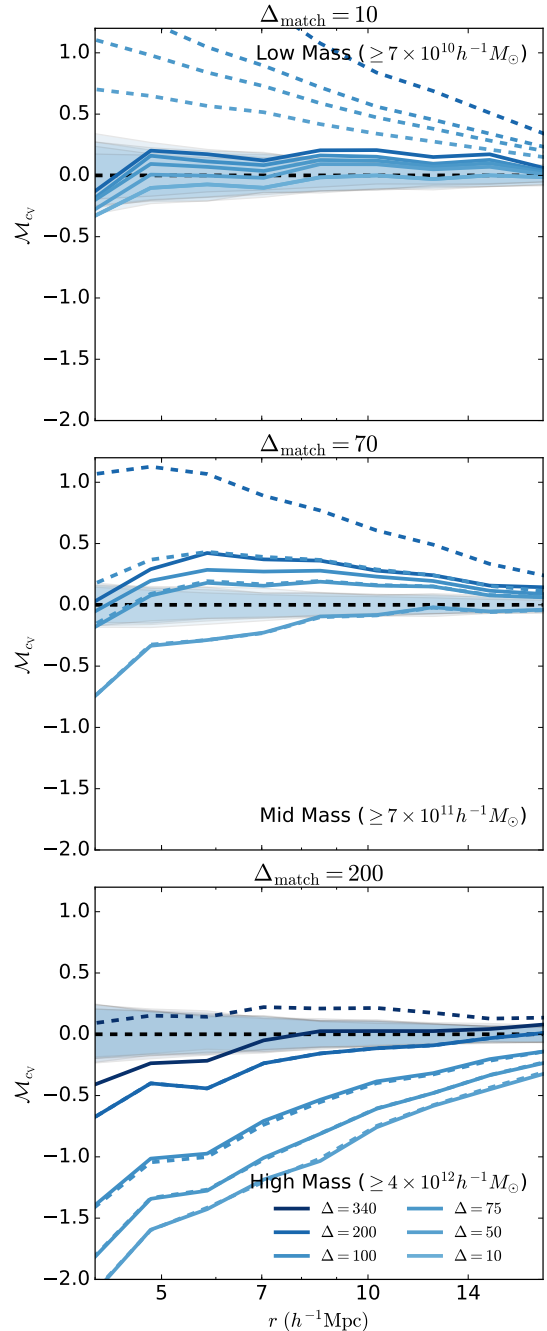

Figure 17. The marked correlation function for the velocity ratio defined halo concentration parameter. The solid lines plot the marked correlation function using velocity ratio halo concentration as the mark, for a catalog matched against the best fit Δ shown in red. The dashed lines plot the original marked correlation function results. In each plot the lines correspond to different values of Δ, with dark blue (light blue) corresponding to $\Delta = 340$ ($\Delta = 50$). The red dashed line corresponds to the overdensity chosen for matching as possibly removing assembly bias on most scales. The top (middle/bottom) panel shows the results for the L0125 (L0250/L0500) data set utilizing the low mass (mid mass/high mass) cutoffs. The shaded bands represent 2-sigma confidence regions generated by randomization of the marks.

the simple halo redefinition technique we have suggested, the underlying reasons for this behavior remains of interest for exploration. In the case of halo shape, we suggest that the assembly bias may be driven through interactions with large scale structure. Studies have shown a statistically significant alignment between filaments and satellite galaxy position (Tempel et al. 2015; Velliscig et al. 2015)[ASV: need to grab paper from arxiv 2016.05.09 for this].

Note that the mass dependence of assembly bias is implicitly explored with our suite of simulations. The nature of the MCFs emphasizes halos just above the threshold mass; e.g. L0125 probes the smallest mass halos, while L0250 probes the largest mass halos. To more explicitly explore this mass dependence, Figure 18 demonstrates how bias scales as a function of both fixed halo mass and choice of overdensity Δ. Here we calculate the bias as follows:

$$b^2(r) = \xi_{c_{\mathrm{NFW}}}/\xi_{\mathrm{all}}, \qquad (8)$$

where $\xi_{c_{\mathrm{NFW}}}$ consists of those halos with the 20% highest marks in NFW-defined concentration and ξ_{all} consists of all halos. Note that due to the limited number of halos in each mass bin, we choose not to use the binning and rank weighting that is utilized in previous analysis. [ASV: This is currently how it is run and I am not sure if this is the best approach. We could probably afford to use 5 bins and it would be a little more fine than when we carry out the full analysis.] To explore the mass dependency of the bias, we choose to examine a fixed scale of 5 to 10 h^{-1}Mpc. We calculate the bias using halos in bins of fixed mass, with errors calculated using resampling in which ξ_{all} is replaced with the correlation function calculated using a randomly chosen subsample of equal number to the biased subsample. The displayed error bars represent the region in which 68% of these random subsamples lie. We explore our dataset with the following binning, in which the larger simulations are able to push to higher masses than the smallest simulation: $7 \times 10^{10} - 2 \times 10^{10}, 2 \times 10^{10} - 7 \times 10^{11}, 7 \times 10^{11} - 2 \times 10^{12}, 2 \times 10^{12} - 7 \times 10^{12}, 7 \times 10^{12} - 2 \times 10^{13}, 2 \times 10^{13} - 7 \times 10^{13}, 7 \times 10^{13} - 2 \times 10^{14} \ h^{-1}M_\odot$.

There are two clear trends to be determined from this data. The first is the trend for the assembly bias with halo concentration to be reduced as a function of halo mass. This trend helps to resolve the apparent inconsistencies in measures of assembly bias in the literature; namely, a change in halo mass of interest can lead to a considerably different measure of halo assembly bias - at high masses, halo assembly bias due to NFW-defined concentration is fairly minimal. The second visible trend is that a change in halo definition chosen has a trend of decreasing the halo bias determined. Furthermore, it should be noted that this can lead to an anticlustering of halos of high concentration at high masses. These two discoveries seem to suggest that halo assembly bias of NFW-defined halo concentration is a coincidence; choosing a halo size across all halo masses as a function of an overdensity will be insufficient in creating self-similiar dark matter halos. [ARZ: Instead, add one summarizing paragraph here discussing the mass dependence of assembly bias. Emphasize that our findings suggest that the strength of assembly bias can be a strong function of halo definition and that this may already be making it difficult to compare the results
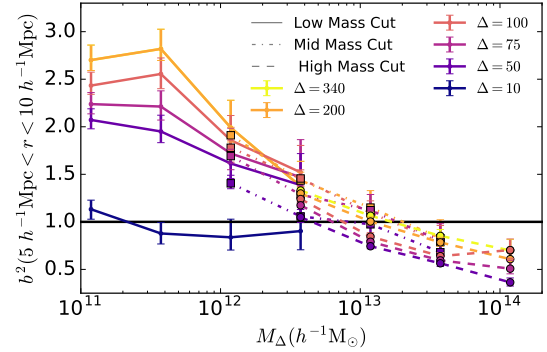

Figure 18. [ARZ: This figure needs to be much bigger in order to be visible. Also, don't use yellow. It's invisible on most screens and is a really bad choice. Basically, do whatever you need to do to keep the basic information, while making the figure trivially readable! You probably only need error bars on one line for each simulation because the error bars are all similar!] [ARZ: In the caption, you need to say what this is the bias of, namely the top 20% in concentration.] [ARZ: Also, can you please make the same figure with the lowest 20%?] [ASV: I can and will be changing this plot - this has been primarily put off due to the fact that this is by far the largest calculation time plot and I wanted to sort out any kinks. I'll cut out all but one error bar and rerun with new colors.] The bias of the 20% highest concentration sample to the full sample, plotted against halo mass measured at the halo radius. The halo mass binning is defined in full detail in the text. Halo definitions descend from the largest definition to lowest definition, from dark to light in color. The dark blue (light blue) line uses a halo definition drawn from $\Delta = 340$ ($\Delta = 50$). The solid (dot-dashed, dashsed) lines use host halos from the L0125(L0250,L0500) catalogs. The error bars encompass 68% of measurements using two hundred subsamples of the mark of the same size as the biased sample. The solid black line shows where there is no detected assembly bias driven by NFW-defined halo concentration.

of various different research groups using different halo definitions.]

7 CONCLUSIONS

[ARZ: After dealing with the comments above, let's come back to rewriting the conclusions section.] We have looked at how to use CFs and MCFs in order to analyze the environmental effects upon the properties of the halo. We have suggested a method of removing the mass dependence that is not subject to the small number statistics at large halo masses. Taking our various tests, we then apply a change to the threshold density Δ in an attempt to remove the effect that environment has upon these properties. We come to the following conclusions from our simulation data.

• Our halo redefinition method does not cause any substantial breakdown in the ROCKSTAR halo finding algorithm, though this may not be the case for every halo finding methodology. This is something that should be considered prior to utilization of this method, unless working directly from particle data. As our initial halo sizes and locations are determined through spherical overdensities, it cannot be assumed that starting from a FoF grouping and then de-

termining values through particle data directly will produce identical results. Similarly, different cosmologies may remove environmental effects at different scales.

• When looking at the two-point correlation function, there appears to be a "sweet spot" that appears to remove environmental effects the most efficiently. Going beyond that seems to reintroduce environmental effects, possibly as an extreme side effect of halo exclusion.

• For our marked correlation functions we see that both proxies of concentration that we use as marks show significant removal of environmental effects at large scales for similar values of the overdensity parameter Δ. In cases where one is only interested in the concentration of dark matter halos and large scales (or correspondingly small values of k), this method will allow you to compensate for bias that environment could introduce to calculations dependent upon the halo model. This may prove valuable for calculations such as that of the shear power spectrum calculated through weak lensing.

• The environmental effects on the shape of the host halo and the satellite number of the host halo cannot be removed regardless of the chosen redefinition of Δ. We propose that this may be intrinsically tied to the nature of the filaments, whose effects cannot be removed by a simple redefinition of the halo radius.

• This method is definitively related to the mass of the halos that are being observed. Furthermore, it appears that the majority of the reduction in assembly bias is tied to the exclusion of halos from the catalog as a result of being subsumed into larger halos. This information does not seem to be contradictory; it can be intuitively understood that the region about the most massive halos will be different than the region around the least massive halos, leading to a different frequency at which halos are being excluded. It does however warrant that careful consideration be given to the sample of halos that are of interest.

• The selection of halo size is intrinsically related to the assembly bias and varies across scales. This might help to resolve contradictory results in the search for halo assembly bias in the literature.

This methodology, while certainly not perfect in accounting for assembly bias, may be of significance when applied to galaxy formation models and give insight into seemingly conflicting results. Provided that the properties of interest in a given model behave well under our redefinition, it will allow us to create better mock galaxy catalogs without resorting to more complicated models requiring halo formation histories - giving us another powerful tool to test observation against.

There remain possible uncertainties to study in the future. One possible area of follow-up is the matter of simulation cosmology, which is not explored in this text. It is possible that the choice of cosmology may change observed assembly bias as a function of the halo masses, something that our methodology should be capable of observing. Furthermore, we can determine if the choice of halo size that best reduces assembly bias is a function of the chosen cosmology. This may be of interest in attempting to determine signatures of assembly bias in observational samples in the future.

REFERENCES

Adhikari S., Dalal N., Chamberlain R. T., 2014, J. Cosm. Astropart. Phys., 11, 019

Allgood B., Flores R. A., Primack J. R., Kravtsov A. V., Wechsler R. H., Faltenbacher A., Bullock J. S., 2006, MNRAS , 367, 1781

Astropy Collaboration et al., 2013, Astron. & Astrophys. , 558, A33

Behroozi P. S., Wechsler R. H., Wu H.-Y., 2013a, Astrophys. J. , 762, 109

Behroozi P. S., Wechsler R. H., Conroy C., 2013b, Astrophys. J. , 770, 57

Bett P., Eke V., Frenk C. S., Jenkins A., Helly J., Navarro J., 2007, MNRAS , 376, 215

Blumenthal G. R., Faber S. M., Primack J. R., Rees M. J., 1984, Nature , 311, 517

Bullock J. S., Wechsler R. H., Somerville R. S., 2002, MNRAS , 329, 246

Cacciato M., van den Bosch F. C., More S., Mo H., Yang X., 2013, MNRAS , 430, 767

Chaves-Montero J., Angulo R. E., Schaye J., Schaller M., Crain R. A., Furlong M., Theuns T., 2016, MNRAS , 460, 3100

Conroy C., Wechsler R. H., 2009, Astrophys. J. , 696, 620

Croton D. J., Gao L., White S. D. M., 2007, MNRAS , 374, 1303

Dalal N., White M., Bond J. R., Shirokov A., 2008, Astrophys. J. , 687, 12

Despali G., Giocoli C., Bonamigo M., Limousin M., Tormen G., 2016, preprint, (`arXiv:1605.04319`)

Diemer B., Kravtsov A. V., 2014, Astrophys. J. , 789, 1

Diemer B., Kravtsov A. V., 2015, Astrophys. J. , 799, 108

Duffy A. R., Schaye J., Kay S. T., Dalla Vecchia C., 2008, MNRAS , 390, L64

Faltenbacher A., White S. D. M., 2010, Astrophys. J. , 708, 469

Fisher J. D., Faltenbacher A., 2016, preprint, (`arXiv:1603.06955`)

Gao L., White S. D. M., 2007, MNRAS , 377, L5

Gao L., White S. D. M., Jenkins A., Frenk C. S., Springel V., 2005, MNRAS , 363, 379

Gil-Marín H., Jimenez R., Verde L., 2011, MNRAS , 414, 1207

Guo Q., et al., 2011, MNRAS , 413, 101

Guo H., et al., 2014, MNRAS , 441, 2398

Hahn O., Porciani C., Carollo C. M., Dekel A., 2007a, MNRAS , 375, 489

Hahn O., Carollo C. M., Porciani C., Dekel A., 2007b, MNRAS , 381, 41

Harker G., Cole S., Helly J., Frenk C., Jenkins A., 2006, MNRAS , 367, 1039

Hearin A., et al., 2016a, preprint, (`arXiv:1606.04106`)

Hearin A. P., Zentner A. R., van den Bosch F. C., Campbell D., Tollerud E., 2016b, MNRAS , 460, 2552

Hunter J. D., 2007, Computing In Science & Engineering, 9, 90

Kazantzidis S., Zentner A. R., Kravtsov A. V., 2006, Astrophys. J. , 641, 647

Lacerna I., Padilla N., 2011, MNRAS , 412, 1283

Leauthaud A., et al., 2012, Astrophys. J. , 744, 159

Li Y., Mo H. J., Gao L., 2008, MNRAS , 389, 1419

Mao Y.-Y., Williamson M., Wechsler R. H., 2015, Astrophys. J. , 810, 21

Mo H., van den Bosch F. C., White S., 2010, Galaxy Formation and Evolution

More S., van den Bosch F. C., Cacciato M., More A., Mo H., Yang X., 2013, MNRAS , 430, 747

More S., Diemer B., Kravtsov A. V., 2015, Astrophys. J. , 810, 36

Moster B. P., Naab T., White S. D. M., 2013, MNRAS , 428, 3121

Navarro J. F., Frenk C. S., White S. D. M., 1997, Astrophys. J. , 490, 493

Peacock J. A., Smith R. E., 2000, MNRAS , 318, 1144

Peebles P. J. E., 1969, Astrophys. J. , 155, 393

Porciani C., Norberg P., 2006, MNRAS , 371, 1824

Rodríguez-Puebla A., Drory N., Avila-Reese V., 2012, Astrophys. J. , 756, 2

Sheth R. K., 2005, MNRAS , 364, 796

Sheth R. K., Tormen G., 2004, MNRAS , 350, 1385

Sunayama T., Hearin A. P., Padmanabhan N., Leauthaud A., 2016, MNRAS , 458, 1510

Tempel E., Guo Q., Kipper R., Libeskind N. I., 2015, preprint, (arXiv:1502.02046)

Tinker J. L., Weinberg D. H., Zheng Z., Zehavi I., 2005, Astrophys. J. , 631, 41

Tinker J. L., Leauthaud A., Bundy K., George M. R., Behroozi P., Massey R., Rhodes J., Wechsler R. H., 2013, Astrophys. J. , 778, 93

Valluri M., Vass I. M., Kazantzidis S., Kravtsov A. V., Bohn C. L., 2007, Astrophys. J. , 658, 731

Velliscig M., et al., 2015, preprint, (arXiv:1504.04025)

Wake D. A., et al., 2011, Astrophys. J. , 728, 46

Walt S. v. d., Colbert S. C., Varoquaux G., 2011, Computing in Science and Engg., 13, 22

Wang H. Y., Mo H. J., Jing Y. P., 2007, MNRAS , 375, 633

Warnick K., Knebe A., Power C., 2008, MNRAS , 385, 1859

Wechsler R. H., Bullock J. S., Primack J. R., Kravtsov A. V., Dekel A., 2002, Astrophys. J. , 568, 52

Wechsler R. H., Zentner A. R., Bullock J. S., Kravtsov A. V., Allgood B., 2006, Astrophys. J. , 652, 71

Wetzel A. R., Nagai D., 2015, Astrophys. J. , 808, 40

Wetzel A. R., Tinker J. L., Conroy C., van den Bosch F. C., 2014, MNRAS , 439, 2687

White S. D. M., Rees M. J., 1978, MNRAS , 183, 341

Yang X., Mo H. J., van den Bosch F. C., 2003, MNRAS , 339, 1057

Yang X., Mo H. J., van den Bosch F. C., 2009, Astrophys. J. , 695, 900

Yang X., Mo H. J., Zhang Y., van den Bosch F. C., 2011, Astrophys. J. , 741, 13

Yang X., Mo H. J., van den Bosch F. C., Zhang Y., Han J., 2012, Astrophys. J. , 752, 41

Zehavi I., et al., 2005, Astrophys. J. , 630, 1

Zehavi I., et al., 2011, Astrophys. J. , 736, 59

Zentner A. R., 2007, International Journal of Modern Physics D, 16, 763

Zentner A. R., Berlind A. A., Bullock J. S., Kravtsov A. V., Wechsler R. H., 2005, Astrophys. J. , 624, 505

Zentner A. R., Hearin A. P., van den Bosch F. C., 2014, MNRAS , 443, 3044

Zhao D. H., Mo H. J., Jing Y. P., Börner G., 2003, MNRAS , 339, 12

Zhao D. H., Jing Y. P., Mo H. J., Börner G., 2009, Astrophys. J. , 707, 354

Zheng Z., Coil A. L., Zehavi I., 2007, Astrophys. J. , 667, 760

Zu Y., Mandelbaum R., 2015, MNRAS , 454, 1161

van Daalen M. P., Angulo R. E., White S. D. M., 2012, MNRAS , 424, 2954

van den Bosch F. C., et al., 2007, MNRAS , 376, 841

APPENDIX

One natural question that might arise in the analysis of this work is the nature of the resulting assembly bias trends. Our focus in the main sections of this paper is on the nature of the assembly bias changing as a function of the mass cut chosen. Our conclusions include the fact that there is a strong mass dependence on halo assembly bias that must be accounted for separately depending on the halos of interest in a study. However, while the existence of this trend is clear within our analysis, the determination that this is solely due to the masses of the halos included in our calculation is less clear upon closer inspection. One possibility that might be particularly concerning is the potential that the different simulations have created halos that have fundamentally different clustering and this is leading to the result that we are interpreting as a mass dependence on assembly bias. Thankfully, though our statistics become less meaningful to carry out this calculation, we can carry out a comparison using the same mass cut across two of our simulations, knowing that these will only contain well resolved halos.

While not addressed directly, Figure **??** through Figure **??** contain a demonstration of the result that we are seeking in the left column of panels. The lower left panels show various marks of interest for L0250 using the "mid mass" cut on the data set. In comparison, the upper left panel contains the same marks of interest for the L0125 using the same mass cut. In the latter, there are fewer halos in this mass cut range, as a result of the smaller simulation box size. However, we note that despite the additional noise in the data set, the behavior of the assembly bias measurement is nearly identical within tolerances accounting for differences between simulations and noise. This motivates our conclusion that the driver behind the behavior is the mass cut of the data sets rather than the resolution of the simulation.